This paper appears in Control Engineering Practice (A Journal of IFAC), 2017.
https://doi.org/10.1016/j.conengprac.2017.07.002

Cooperative Modalities in Robotic Tele-Rehabilitation Using Nonlinear Bilateral Impedance Control

Mojtaba Sharifi [a,b], Saeed Behzadipour [a], Hassan Salarieh [a] and Mahdi Tavakoli [b,*]

[a] *Department of Mechanical Engineering, Sharif University of Technology, Tehran, 11155-9567, Iran*
[b] *Department of Electrical and Computer Engineering, University of Alberta, Edmonton, Alberta, T6G 1H9 Canada*

Abstract

A nonlinear model reference adaptive bilateral impedance controller is proposed that can accommodate various cooperative tele-rehabilitation modes for patient-therapist interaction using a multi-DOF tele-robotic system. In this controller, two reference impedance models are implemented for the master and slave robots using new model reference adaptive control laws for the nonlinear bilateral teleoperation system. “Hand-over-hand” and “adjustable-flexibility” are two modes of patient-therapist cooperation that are realized using the proposed strategy. The Lyapunov-based stability proof guarantees the patient’s and the therapist’s safety during the cooperation and interaction with robots, even in the presence of modeling uncertainties of the multi-DOF teleoperation system. The performance of the proposed bilateral impedance controller is experimentally investigated for upper-limb tele-rehabilitation in the two mentioned cooperation modes.

Keywords: Robotic tele-rehabilitation, patient-robot interaction, cooperative therapy, nonlinear adaptive bilateral control, Lyapunov stability.

* Corresponding Author.
E-mails: sharifi3@ualberta.ca (M. Sharifi), behzadipour@sharif.edu (S. Behzadipour), salarieh@sharif.edu (H. Salarieh), mahdi.tavakoli@ualberta.ca (M. Tavakoli).

1. Introduction

Stroke, cerebral palsy, multiple sclerosis, and Parkinson’s disease are some of age-related disorders that cause various forms of disability. The proposed robotics-assisted framework for tele-rehabilitation will be useful for any pathology that impairs motion of a body extremity and necessitates retraining of a function. While the framework proposed in this paper has a wide range of applications, without loss of generality, the discussion in the following focuses on the rehabilitation after stroke as a particular example of such disabilities.

Since the required intensive rehabilitation of patients with disabilities is costly, robotic systems have been developed to provide consistent and reproducible rehabilitation services [1-3]. Different robotic rehabilitation systems have been developed and tested in the past two decades involving only one robot manipulator interacting with the patient’s limb [4-7]. However, to perform rehabilitation tasks with live (online) cooperation or assistance of a therapist, a second robot is needed to capture the therapist’s input. A bilateral teleoperation system can provide a tele-rehabilitation environment that allows the therapist and the patient to interact with each other for various movements and functional therapies.

The concept of tele-rehabilitation using robotic systems has been presented in [8-17]. The unilateral [11, 12] and bilateral [13, 14, 18] systems for tele-rehabilitation rely on a shared

virtual environment (SVE) visible to both the patient and the therapist. Most of these strategies [11-14] have used the two robots positions in the SVE. The interaction force has been also measured in [15, 18] to achieve the force reflecting performance in tele-rehabilitation besides the position tracking performance.

A new trilateral architecture has been suggested in [19, 20] for mirror therapy of the patient's impaired limb using the Guidance Virtual Fixtures (GVFs) concept and incorporating the patient's functional (healthy) limb. In this architecture, the therapist supervised the cooperation of impaired and functional limbs of the patient by generating some corrective movements [20]. Moreover, different multi-agent strategies have been recently studied in [21] for training some trainees by the therapist during the tele-rehabilitation of a patient. Different position and force objectives have been presented in [21] for multilateral (multi-master-slave) systems; however, the impedance adjustment was not studied. In the above-mentioned recent works [19-21], the system uncertainty has not been taken into account, and a nonlinear stability analysis (such as Lyapunov method) has not be employed for the multi-DOF telerobotic system.

Various control methods have been suggested for single-DOF (linear) teleoperation systems [22-25]. However, to perform complex and dexterous therapy exercises, multi-DOF (nonlinear) teleoperation systems are required. Accordingly, some adaptive bilateral control strategies have been proposed to synchronize the positions of nonlinear master and slave robots [26-28]. Also, to achieve both position tracking and force tracking, nonlinear adaptive control methods [29-31] have been developed. The controllers presented in [29-31] require the acceleration signals of the robots, and force tracking is achieved only when the estimates of unknown model parameters converge to the real values; this only happens in the presence of persistent excitations.

Using the impedance/admittance control theory [32-34], interactive rehabilitation tasks were realized for interaction of a patient with a robot [5, 35]; such tasks cannot be performed well by pure position or force control. The impedance control context has been employed for one-DOF linear bilateral teleoperation systems [36-39]. An impedance/admittance model with a damping element for both master and slave robots was defined in [40]. What is still missing is a bilateral impedance control framework for multi-DOF nonlinear teleoperation systems with corresponding nonlinear stability analysis, which is the focus of this paper, aimed at dexterous movements.

In the present work, a new nonlinear adaptive bilateral impedance controller is developed. While the control framework is applicable to general teleoperation systems, in this paper we focus on facilitating two specific modes of patient-therapist cooperation in robotic tele-rehabilitation (item 2 in the list below).

The proposed control framework has the following characteristics:

1) The impedance of the teleoperation system is controlled by enforcing two desired impedance models for the master and slave robots, interacting with the therapist and the patient. This is unlike the previous nonlinear bilateral controllers [29, 31, 41, 42] that have position and force tracking control objectives. In the proposed control strategy, by adjustment of the impedance models, the patient and the therapist are not forced to have the same position as is the objective of traditional PEB (Position Error Based) [25] and DFR (Direct Force Reflection) [43] control strategies for teleoperation systems.

2) Two multi-DOF robotic tele-rehabilitation strategies can be accommodated using the proposed bilateral impedance control framework. The cooperative "hand-over-hand" and "adjustable-flexibility" modes of patient-therapist interaction are achieved through appropriate selection of the two reference impedance models for the master and slave robots.

3) Due to (a) the freedom provided for the patient and the therapist as a result of adjusting the impedance models, (b) the stability of these impedance models, and (c) the Lyapunov-based stability of the entire multi-DOF nonlinear tele-rehabilitation system in the presence of modeling uncertainties, the patient and therapist safety is guaranteed. Patient safety is a critically important issue in robotic tele-rehabilitation [8]. Note that the stability of the multi-DOF

nonlinear telerobotic system was not proven in most of previous studies focusing on tele-rehabilitation applications [9-12].

4) The force and position scaling factors are defined in the proposed impedance models to adjust the haptic force feedback level and to account for possible workspace asymmetries between the master and slave robots. Employing the force scaling, the therapist can sense a scaled-down version of the patient force. Also, using the position scaling, the therapist motion trajectory can be scaled-up for the patient such that the slave robot motion become larger than the master one. As a result of this feature, the therapist fatigue reduces using the proposed robotic tele-rehabilitation strategy in comparison with the direct physical interaction of the patient and the therapist (without employing robots).

5) The proposed bilateral controller is robust against modeling uncertainties in the nonlinear teleoperation system using two adaptation laws for the master and the slave control systems. In addition, unlike the previous nonlinear bilateral adaptive controllers (such as [29, 31, 41]) in which force tracking was achieved only when the estimation of model parameters converged to the real values (persistent excitation condition), the position and force tracking can be obtained simultaneously in the current framework without any requirement on the precise identification of system parameters.

6) The design of proposed control laws for the master and the slave is motivated by a new nonlinear Model Reference Adaptive Impedance Control (MRAIC) scheme presented recently for physical human-robot interaction (involving a single robot but not a teleoperation system) [34]. Since in the MRAIC method, the closed-loop dynamics of the robot is made similar to the reference impedance model which is a stable system, the scheme in [34] is more effective than simple adaptive impedance controllers in realizing the impedance model for a nonlinear manipulator.

The aforementioned characteristics and applications of the proposed bilateral impedance controller are novel in the context of robotic tele-rehabilitation systems.

2. Multi-DOF Robotic Tele-Rehabilitation System

The nonlinear dynamics of an *n*-DOF tele-rehabilitation system (including the master and slave robot manipulators) is introduced in the joint space as [44]:

$$\mathbf{M}_{\mathbf{q},m}(\mathbf{q}_m)\ddot{\mathbf{q}}_m + \mathbf{C}_{\mathbf{q},m}(\mathbf{q}_m,\dot{\mathbf{q}}_m)\dot{\mathbf{q}}_m + \mathbf{G}_{\mathbf{q},m}(\mathbf{q}_m) + \mathbf{F}_{\mathbf{q},m}(\dot{\mathbf{q}}_m) = \boldsymbol{\tau}_m + \boldsymbol{\tau}_{th} \quad (1)$$

$$\mathbf{M}_{\mathbf{q},s}(\mathbf{q}_s)\ddot{\mathbf{q}}_s + \mathbf{C}_{\mathbf{q},s}(\mathbf{q}_s,\dot{\mathbf{q}}_s)\dot{\mathbf{q}}_s + \mathbf{G}_{\mathbf{q},s}(\mathbf{q}_s) + \mathbf{F}_{\mathbf{q},s}(\dot{\mathbf{q}}_s) = \boldsymbol{\tau}_s - \boldsymbol{\tau}_{pa} \quad (2)$$

where $\mathbf{q}_m$ and $\mathbf{q}_s \in \mathbb{R}^{n\times 1}$ are the joint position vectors, $\mathbf{M}_{\mathbf{q},m}(\mathbf{q}_m)$ and $\mathbf{M}_{\mathbf{q},s}(\mathbf{q}_s) \in \mathbb{R}^{n\times n}$ are the inertia or mass matrices, $\mathbf{C}_{\mathbf{q},m}(\mathbf{q}_m,\dot{\mathbf{q}}_m)$ and $\mathbf{C}_{\mathbf{q},s}(\mathbf{q}_s,\dot{\mathbf{q}}_s) \in \mathbb{R}^{n\times n}$ include the centrifugal and Coriolis terms, $\mathbf{G}_{\mathbf{q},m}(\mathbf{q}_m)$ and $\mathbf{G}_{\mathbf{q},s}(\mathbf{q}_s) \in \mathbb{R}^{n\times 1}$ are the gravity terms, $\mathbf{F}_{\mathbf{q},m}(\dot{\mathbf{q}}_m)$ and $\mathbf{F}_{\mathbf{q},s}(\dot{\mathbf{q}}_s) \in \mathbb{R}^{n\times 1}$ are the friction torques, and $\boldsymbol{\tau}_m$ and $\boldsymbol{\tau}_s \in \mathbb{R}^{n\times 1}$ are the vectors of the control torques (from the joint actuators) of the master and the slave robots, respectively. Also, $\boldsymbol{\tau}_{th}$ and $\boldsymbol{\tau}_{pa} \in \mathbb{R}^{n\times 1}$ are the interaction torques that the therapist applies to the master robot and the slave robot applies to the patient, respectively. Then, the robots' end-effector dynamics in the Cartesian space is defined as:

$$\mathbf{M}_{\mathbf{x},m}(\mathbf{q}_m)\ddot{\mathbf{x}}_m + \mathbf{C}_{\mathbf{x},m}(\mathbf{q}_m,\dot{\mathbf{q}}_m)\dot{\mathbf{x}}_m + \mathbf{G}_{\mathbf{x},m}(\mathbf{q}_m) + \mathbf{F}_{\mathbf{x},m}(\dot{\mathbf{q}}_m) = \mathbf{f}_m + \mathbf{f}_{th} \quad (3)$$

$$\mathbf{M}_{\mathbf{x},s}(\mathbf{q}_s)\ddot{\mathbf{x}}_s + \mathbf{C}_{\mathbf{x},s}(\mathbf{q}_s,\dot{\mathbf{q}}_s)\dot{\mathbf{x}}_s + \mathbf{G}_{\mathbf{x},s}(\mathbf{q}_s) + \mathbf{F}_{\mathbf{x},s}(\dot{\mathbf{q}}_s) = \mathbf{f}_s - \mathbf{f}_{pa} \quad (4)$$

where $\mathbf{x}_m$ and $\mathbf{x}_s \in \mathbb{R}^{6\times 1}$ are the position vectors of master and slave robots' end-effectors, respectively, in the Cartesian coordinates. $\mathbf{f}_{th}$ and $\mathbf{f}_{pa} \in \mathbb{R}^{6\times 1}$ are the interaction forces that the therapist applies to the master end-effectors and the slave end-effector applies to the patient, respectively. Considering the subscript $i = m$ for the master and $i = s$ for the slave, kinematic transformations between the joint and Cartesian spaces are presented for each robot as:

$$\mathbf{x}_i = \Omega_i(\mathbf{q}_i),\ \ \dot{\mathbf{x}}_i = \mathbf{J}_i(\mathbf{q}_i)\dot{\mathbf{q}}_i,\ \ \ddot{\mathbf{x}}_i = \mathbf{J}_i(\mathbf{q}_i)\ddot{\mathbf{q}}_i + \dot{\mathbf{J}}_i(\mathbf{q}_i)\dot{\mathbf{q}}_i \quad (5)$$

where $\mathbf{J}_i(\mathbf{q}_i) = d\Omega_i(\mathbf{q}_i)/d\,\mathbf{q}_i$ is the Jacobian matrix. The relations of the dynamic matrices and vectors between the joint space (Eqs. (1) and (2)) and the Cartesian space (Eqs. (3) and (4)) with non-singular Jacobian matrices are expressed as

$$\begin{aligned}
&\mathbf{M}_{\mathbf{x},i}(\mathbf{q}_i) = \mathbf{J}_i^{-T}\mathbf{M}_{\mathbf{q},i}(\mathbf{q}_i)\mathbf{J}_i^{-1}, \quad \mathbf{G}_{\mathbf{x},i}(\mathbf{q}_i) = \mathbf{J}_i^{-T}\mathbf{G}_{\mathbf{q},i}(\mathbf{q}_i) \\
&\mathbf{C}_{\mathbf{x},i}(\mathbf{q}_i,\dot{\mathbf{q}}_i) = \mathbf{J}_i^{-T}\left(\mathbf{C}_{\mathbf{q},i}(\mathbf{q}_i,\dot{\mathbf{q}}_i) - \mathbf{M}_{\mathbf{q},i}(\mathbf{q}_i)\mathbf{J}_i^{-1}\dot{\mathbf{J}}_i\right)\mathbf{J}_i^{-1} \\
&\mathbf{F}_{\mathbf{x},i}(\mathbf{q}_i) = \mathbf{J}_i^{-T}\mathbf{F}_{\mathbf{q},i}(\mathbf{q}_i), \quad \mathbf{f}_i = \mathbf{J}_i^{-T}\boldsymbol{\tau}_i \\
&\mathbf{f}_{th} = \mathbf{J}_m^{-T}\boldsymbol{\tau}_{th}, \quad \mathbf{f}_{pa} = \mathbf{J}_s^{-T}\boldsymbol{\tau}_{pa}
\end{aligned} \tag{6}$$

These matrices and vectors have following properties [43-45]:

Property 1. *The left side of Eqs. (1) and (2) is linearly parameterized as:*

$$\begin{aligned}
&\mathbf{M}_{\mathbf{q},i}(\mathbf{q}_i)\boldsymbol{\varphi}_{\mathbf{1},i} + \mathbf{C}_{\mathbf{q},i}(\mathbf{q}_i,\dot{\mathbf{q}}_i)\boldsymbol{\varphi}_{\mathbf{2},i} + \mathbf{G}_{\mathbf{q},i}(\mathbf{q}_i) + \mathbf{F}_{\mathbf{q},i}(\dot{\mathbf{q}}_i) \\
&\qquad = \mathbf{Y}_{\mathbf{q},i}(\boldsymbol{\varphi}_{\mathbf{1},i}, \boldsymbol{\varphi}_{\mathbf{2},i}, \mathbf{q}_i, \dot{\mathbf{q}}_i)\boldsymbol{\alpha}_{\mathbf{q},i}
\end{aligned} \tag{7}$$

where $\boldsymbol{\alpha}_{\mathbf{q},i}$ is the vector of unknown parameters of the robot. The regressor matrix $\mathbf{Y}_{\mathbf{q},i}$ contains known functions [44] in terms of the arbitrary vectors $\boldsymbol{\varphi}_{\mathbf{1},i}$ and $\boldsymbol{\varphi}_{\mathbf{2},i}$.

Property 2. $\dot{\mathbf{M}}_{\mathbf{q},i}(\mathbf{q}_i) - 2\mathbf{C}_{\mathbf{q},i}(\mathbf{q}_i,\dot{\mathbf{q}}_i)$ *and* $\dot{\mathbf{M}}_{\mathbf{x},i}(\mathbf{q}_i) - 2\mathbf{C}_{\mathbf{x},i}(\mathbf{q}_i,\dot{\mathbf{q}}_i)$ *are skew symmetric matrices.*

Property 3. $\mathbf{M}_{\mathbf{q},i}(\mathbf{q}_i)$ *and* $\mathbf{M}_{\mathbf{x},i}(\mathbf{q}_i)$ *are symmetric positive definite matrices.*

3. Tele-Rehabilitation Objectives in Bilateral Impedance Control

In the proposed bilateral tele-rehabilitation system, two impedance models are defined for the master and slave robots interacting with the therapist and patient, respectively. For this purpose, the position and velocity signals of the master robot and the master/therapist interaction force are transmitted to the patient site for use in the slave robot's impedance model and controller. Also, the patient-slave interaction force is transmitted to the therapist site to be employed in the master impedance model and controller. The impedance concepts and transmitted signals are schematically shown in Fig. 1 where $\mathbf{x}_{\mathrm{mod}_m}$ and $\mathbf{x}_{\mathrm{mod}_s}$ are the desired impedance responses of the master and slave, respectively.

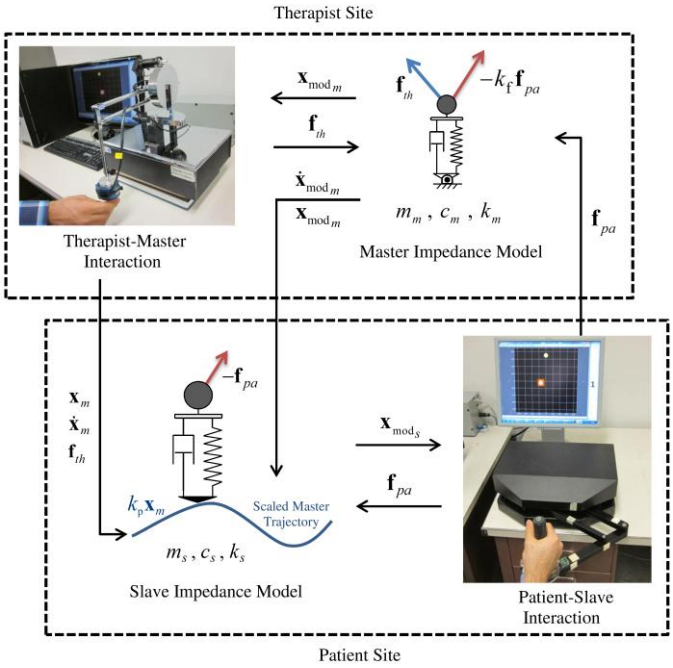

Fig. 1. The proposed bilateral tele-rehabilitation system with separate impedance models for the master and the slave.

3.1. Position and Force Scaling

As illustrated in Fig. 1, the motion of the therapist's limb (in this case, his/her hand), which is equal to the master position, is scaled by k_{p} during transmission while the patient/slave contact force is scaled by k_{f} during transmission and before being used in the impedance model and the controller at the destination,

$$\mathbf{x}_{m_{scaled}} = k_{\mathrm{p}}\,\mathbf{x}_m, \quad \mathbf{f}_{pa_{scaled}} = k_{\mathrm{f}}\,\mathbf{f}_{pa} \tag{8}$$

This scaling feature is useful when the workspaces and force rendering capabilities of the master and slave robots are different. Also, if the patient force is scaled down for the therapist ($k_{\mathrm{f}} < 1$), the therapist can work with a lightweight master robot such as a standard haptic device with relatively low force rendering capability. In this case, the therapist's fatigue is reduced as well.

3.2. Master and Slave Impedance Models

The desired impedance model of the master robot defines a dynamical relationship between a linear combination of the therapist/master contact force $\mathbf{f}_{th}$ and the patient/slave contact force $\mathbf{f}_{pa}$ and the desired master robot trajectory in Cartesian

space $\mathbf{x}_{\mathrm{mod}_m}$:

$$m_m \ddot{\mathbf{x}}_{\mathrm{mod}_m} + c_m \dot{\mathbf{x}}_{\mathrm{mod}_m} + k_m \mathbf{x}_{\mathrm{mod}_m} = \mathbf{f}_{th} - k_{\mathrm{f}} \mathbf{f}_{pa} \quad (9)$$

where m_m , c_m and k_m are the desired virtual mass, damping and stiffness parameters of the master impedance model, respectively. In order to have different impedance characteristics in different directions, these parameters can be replaced by matrices. The factor k_{f} in (9) scales the patient force $\mathbf{f}_{pa}$, as it is transmitted for reflection to the therapist. According to Eq. (9), when the master robot controller reaches its objective, which is tracking the master impedance model's response $\mathbf{x}_{\mathrm{mod}_m}$, the therapist senses a scaled version of the patient force $\mathbf{f}_{pa}$.

The desired impedance model of the slave robot is expressed as a dynamic relationship between the patient force $\mathbf{f}_{pa}$ and the desired difference, $\tilde{\mathbf{x}}_{\mathrm{mod}_s} = \mathbf{x}_{\mathrm{mod}_s} - k_{\mathrm{p}} \mathbf{x}_m$, between the slave and the scaled master positions:

$$m_{\mathrm{s}} \ddot{\tilde{\mathbf{x}}}_{\mathrm{mod}_s} + c_{\mathrm{s}} \dot{\tilde{\mathbf{x}}}_{\mathrm{mod}_s} + k_{\mathrm{s}} \tilde{\mathbf{x}}_{\mathrm{mod}_s} = -\mathbf{f}_{pa} \quad (10)$$

where m_s , c_s and k_s are the desired virtual mass, damping, and stiffness parameters of the slave impedance model.

Accordingly, two impedance models are defined in this framework. The first one is the master impedance model (9) perceived by both the therapist and the patient. The second one is the slave impedance model (10) that determines the freedom of patient in terms of deviating away from the therapist-commanded trajectory (i.e., the master trajectory) by applying forces to the slave robot. The applications of the proposed desired impedance models are further explained in the next sections for cooperative tele-rehabilitation strategies.

Both impedance models for the master (9) and the slave (10) are stable second-order differential equations when using positive mass, damping and stiffness parameters. Therefore, bounded input forces of the patient $\mathbf{f}_{pa}$ and therapist $\mathbf{f}_{th}$ will not generate unbounded desired trajectories for the robots. This characteristic of reference impedance models is a prerequisite for the safety of the patient and the therapist.

3.3. "Hand-Over-Hand" Cooperative Tele-Rehabilitation Mode

The "hand-over-hand" cooperative tele-rehabilitation mode corresponds to the case where the therapist and the patient, who are controlling the master and the slave respectively, feel as if they are interacting with each other directly and kinesthetically in a fashion similar to the traditional physical hand-over-hand therapy [8]. This happens under full transparency (i.e., both perfect position tracking and perfect force tracking). The therapist and the patient will sense the force of each other (except for a possible scaling) and have the same position (except for a possible scaling), facilitating their cooperation.

The proposed bilateral impedance control strategy can ensure the perfect position tracking performance and/or the exact force reflection performance by suitable adjustment of the parameters in the two impedance models (10) and (9), respectively. In the master impedance model (9), $\mathbf{x}_{\mathrm{mod}_m}$, $\dot{\mathbf{x}}_{\mathrm{mod}_m}$ and $\ddot{\mathbf{x}}_{\mathrm{mod}_m}$ are bounded at the left side due to the bounded interaction forces $\mathbf{f}_{th}$ and $\mathbf{f}_{pa}$ at the right side. Thus, by choosing small values for the parameters m_m , c_m and k_m , the left side of (9) can be made arbitrarily small based on the boundedness of $\mathbf{x}_{\mathrm{mod}_m}$, $\dot{\mathbf{x}}_{\mathrm{mod}_m}$ and $\ddot{\mathbf{x}}_{\mathrm{mod}_m}$. This results in $(\mathbf{f}_{th} - k_{\mathrm{f}} \mathbf{f}_{pa}) \to 0$ at the right side of (9), i.e., scaled force reflection is achieved. Moreover, due to the boundedness of the right side of (10), which is the negative of the patient force, the left side of this equation is also bounded. Consequently, employing large enough values for the slave impedance parameters (m_s , c_s and k_s) in (10) can make the tracking error $\tilde{\mathbf{x}}_{\mathrm{mod}_s}$ arbitrarily small, and the position tracking performance ($\mathbf{x}_{\mathrm{mod}_s} \to k_p \mathbf{x}_m$) is obtained.

In such a setting, it seems as if the therapist is rigidly holding the patient's arm during the motion (i.e., they experience the same motion if the position scaling factor is unity) and feel each other's force if the force scaling factor is unity. However, as the patient capabilities are improved, his/her freedom to follow the therapist's motion or deviate from it should increase as discussed in the next subsection.

3.4. "Adjustable-Flexibility" Cooperative Tele-Rehabilitation Mode

In this cooperative rehabilitation modality, the patient is aided to complete a desired task with an adjustable compliance (flexibility to deviate from the therapist position). The level of this flexibility can be adjusted by the therapist according to the stage of the rehabilitation process, the patient's improvement so far, and the patient's engagement [1]. Such flexibility has been achieved through impedance control [32] in rehabilitation systems with one robotic manipulator [5].

The "adjustable-flexibility" mode of cooperation between the therapist and the patient is realized in the proposed tele-rehabilitation system by selecting the parameters of the slave impedance model to have moderate values based on the therapist's opinion and the patient's motor performance. In other words, the slave impedance parameters (m_s, c_s and k_s in (10)) are chosen to be smaller than those used in the "hand-over-hand" cooperative tele-rehabilitation mode (Sec. 3.3) to provide a level of compliance for the patient in deviating ($\tilde{\mathbf{x}}_{\mathrm{mod}_s}$) from the therapist's trajectory. By decreasing the slave impedance model parameters, the level of assistance provided to the patient is also reduced. Therefore, as the patient capabilities are improved and his/her success level in doing the rehabilitation exercises increases, the slave impedance parameters should be further decreased for realizing assist-as-needed therapy.

Another assistance mechanism for the patient is through applying forces $\mathbf{f}_{th}$ by the therapist, which through (9) assist the patient to move in the required direction.

While the slave impedance model was used to deliver flexibility (compliance) to the patient, the master impedance model can be used to ensure a perfect force reflection performance ($(\mathbf{f}_{th} - k_{\mathrm{f}}\mathbf{f}_{pa}) \to 0$). To this end, the master impedance parameters m_m, c_m and k_m in (9) are considered to be small similar to the previous Sec. 3.3.

The achievable patient-therapist cooperative modes in a tele-rehabilitation context using the proposed bilateral impedance control framework and the guidelines on selection of parameters in the master and slave impedance models (9) and (10) are summarized in Table 1, which were discussed in Sec. 3.3 and Sec. 3.4.

Table 1. Adjustment of parameters in master and slave impedance models for cooperative tele-rehabilitation modes

Cooperative Tele-Rehab. Mode	Master Imp. Model Parameters m_m, c_m, k_m	Slave Imp. Model Parameters m_s, c_s, k_s	Scaling Factor† k_{f}
Hand-Over-Hand (Sec. 3.3)	Small*	Large*	Small, e.g.: $1 \geq k_{\mathrm{f}} \geq 1/4$
Adjustable-Flexibility (Sec. 3.4)	Small*	Moderate*	Small, e.g.: $1 \geq k_{\mathrm{f}} \geq 1/4$

* Some sample ranges for the small, moderate and large values of the stiffness parameter are respectively suggested as $k_i < 10$ N/m, 50 N/m $< k_i < 200$ N/m and 1000 N/m $< k_i$ for each of the master ($i = m$) and the slave ($i = s$) impedance models. It should be noted that the suggested sample ranges also depend on the patient's and therapist's haptic senses, and they can be adjusted by an initial trial and error process. Moreover, the damping c_i and mass m_i parameters of each impedance model can be adjusted based on the stiffness parameter k_i and other characteristics such as the natural frequency $\omega_{n_i} = \sqrt{k_i/m_i}$ and the damping ratio $\zeta_i = c_i/2\sqrt{m_i k_i}$ of the impedance model, as will be described in the experimental implementations (Sec. 6).

† A sample value is suggested for the force scaling factor (k_{f}), which can be changed based on the specified force scaling requirements. Also, the position scaling factor (k_{p}) should be chosen based on the workspace size of the master and slave robots and/or any other specific requirements for scaling the therapist and patient motions.

4. Nonlinear Bilateral Model Reference Adaptive Control Laws

The architecture of the proposed nonlinear bilateral impedance controller is shown in Fig. 2 and its details are given in this section. As mentioned earlier, there are two reference impedance models (9) and (10) that are realized for the master and slave robots by nonlinear bilateral model reference adaptive impedance controller. The dynamic models of the master and slave robots are considered to have parametric modeling uncertainties. Moreover, the interaction forces of the therapist and patient ($\mathbf{f}_{th}$ and $\mathbf{f}_{pa}$) applied to robots are measured using force sensors attached to the master and slave end-effectors, respectively.

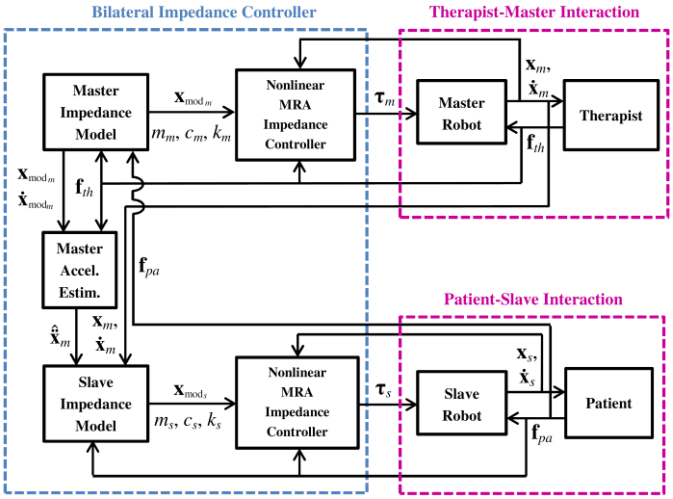

Fig. 2. Architecture of the nonlinear adaptive bilateral impedance controller for tele-rehabilitation systems.

The nonlinear adaptive control laws of the master and slave robots are developed according to the new nonlinear Model Reference Adaptive Impedance control (MRAIC) scheme [34] presented for one robot. Since the closed-loop dynamics of the system (robot) is made similar to the stable reference impedance model in the MRAIC method, it was shown that the MRAIC scheme [34] is more effective than other simple adaptive controllers (e.g., [46]) that only track the response of the impedance model. Now, for the current bilateral tele-rehabilitation system, the master ($i=m$) and slave ($i=s$) reference impedance models (9) and (10) are stable, and each of them has two poles with negative real parts:

$$r_{1,i}=-\lambda_{1,i}+j\,\lambda_{3,i}\ ,\quad r_{2,i}=-\lambda_{2,i}-j\,\lambda_{3,i} \tag{11}$$

where $\lambda_{1,i}$ and $\lambda_{2,i}$ are both positive constants and ensure the stability of the reference impedance models. Due to the design of the impedance parameters in Eqs. (9) and (10), two cases are possible for the stable poles in Eq. (11): 1) two conjugate complex poles with the same negative real part ($\lambda_{1,i}=\lambda_{2,i}$ and $\lambda_{3,i}\neq 0$), and 2) two non-equal negative real poles ($\lambda_{1,i}\neq\lambda_{2,i}$ and $\lambda_{3,i}=0$). Therefore, employing the master and slave impedance dynamics (9) and (10) and their poles, one can write:

$$\begin{aligned}\left((d/dt)+\lambda_{1,m}-j\lambda_{3,m}\right)\left((d/dt)+\lambda_{2,m}+j\lambda_{3,m}\right)\tilde{\mathbf{x}}_m=\\ \ddot{\tilde{\mathbf{x}}}_m+\left(c_m/m_m\right)\dot{\tilde{\mathbf{x}}}_m+\left(k_m/m_m\right)\tilde{\mathbf{x}}_m\\ \left((d/dt)+\lambda_{1,s}-j\lambda_{3,s}\right)\left((d/dt)+\lambda_{2,s}+j\lambda_{3,s}\right)\tilde{\mathbf{x}}_s=\\ \ddot{\tilde{\mathbf{x}}}_s+\left(c_s/m_s\right)\dot{\tilde{\mathbf{x}}}_s+\left(k_s/m_s\right)\tilde{\mathbf{x}}_s\end{aligned} \tag{12}$$

where $\tilde{\mathbf{x}}_m=\mathbf{x}_m-\mathbf{x}_{\mathrm{mod}_m}$ and $\tilde{\mathbf{x}}_s=\mathbf{x}_s-\mathbf{x}_{\mathrm{mod}_s}$ are the vectors of the master and slave position errors with respect to the responses of their impedance models (9) and (10). Now, since the controller benefits from the stability characteristics of the reference impedance models based on the MRAIC theory [34], the sliding surfaces are designed due to the stable poles (11):

$$\begin{aligned}\mathbf{s}_m&=\left((d/dt)+\lambda_{1,m}\right)\tilde{\mathbf{x}}_m=\dot{\tilde{\mathbf{x}}}_m+\lambda_{1,m}\tilde{\mathbf{x}}_m,\\ \mathbf{s}_s&=\left((d/dt)+\lambda_{1,s}\right)\tilde{\mathbf{x}}_s=\dot{\tilde{\mathbf{x}}}_s+\lambda_{1,s}\tilde{\mathbf{x}}_s,\end{aligned} \tag{13}$$

Regarding Eqs. (13) and (12), one can write:

$$\begin{aligned}\ddot{\tilde{\mathbf{x}}}_m+\left(c_m/m_m\right)\dot{\tilde{\mathbf{x}}}_m+\left(k_m/m_m\right)\tilde{\mathbf{x}}_m-\lambda_{3,m}^2\tilde{\mathbf{x}}_m=\\ \left((d/dt)+\lambda_{2,m}\right)\mathbf{s}_m\\ \ddot{\tilde{\mathbf{x}}}_s+\left(c_s/m_s\right)\dot{\tilde{\mathbf{x}}}_s+\left(k_s/m_s\right)\tilde{\mathbf{x}}_s-\lambda_{3,s}^2\tilde{\mathbf{x}}_s=\\ \left((d/dt)+\lambda_{2,s}\right)\mathbf{s}_s\end{aligned} \tag{14}$$

Accordingly, the master and slave reference velocities are defined as:

$$\dot{\mathbf{x}}_{\mathbf{r},m}=\dot{\mathbf{x}}_{\mathrm{mod}_m}-\lambda_{1,m}\tilde{\mathbf{x}}_m\ ,\quad \dot{\mathbf{x}}_{\mathbf{r},s}=\dot{\mathbf{x}}_{\mathrm{mod}_s}-\lambda_{1,s}\tilde{\mathbf{x}}_s \tag{15}$$

such that the sliding surfaces can be reformulated as $\mathbf{s}_m=\dot{\mathbf{x}}_m-\dot{\mathbf{x}}_{\mathbf{r},m}$ and $\mathbf{s}_s=\dot{\mathbf{x}}_s-\dot{\mathbf{x}}_{\mathbf{r},s}$.

Since the acceleration of the master robot ($\ddot{\mathbf{x}}_m$) is required in the slave controller and its measurement is challenging, it is estimated with a good accuracy when the master robot mimics its impedance model (9). In other words, the master end-effector acceleration ($\ddot{\mathbf{x}}_m$) is estimated from Eq. (9), as:

$$\begin{aligned}\hat{\ddot{\mathbf{x}}}_m&=m_m^{-1}\left(\mathbf{f}_{th}-k_{\mathrm{f}}\mathbf{f}_{pa}\right)\\ &\quad-m_m^{-1}c_m\dot{\mathbf{x}}_{\mathrm{mod}_m}-m_m^{-1}k_m(\mathbf{x}_{\mathrm{mod}_m}-\mathbf{x}_0)\end{aligned} \tag{16}$$

Therefore, when the master robot trajectory $\mathbf{x}_m$ converges to the master impedance model response $\mathbf{x}_{\mathrm{mod}_m}$, the accuracy of Eq. (16) in estimation of the master acceleration increases.

Due to the physical assumption that the therapist and the patient cannot generate unbounded forces during their interaction with robots, $\mathbf{f}_{th}$ and $\mathbf{f}_{pa}$ are considered bounded in Eqs. (9), (10) and (16). Thus, $\dot{\mathbf{x}}_{\mathrm{mod}_m}$ and $\mathbf{x}_{\mathrm{mod}_m}$ as the response of the master impedance model (9) are bounded, and consequently the obtained master acceleration estimation $\hat{\ddot{\mathbf{x}}}_m$ from Eq. (16) remains bounded. Using the estimation of master robot acceleration (16), the measured therapist force ($\mathbf{f}_{th}$) together with the master robot trajectory ($\mathbf{x}_m$ and $\dot{\mathbf{x}}_m$) and the master impedance model's trajectory ($\mathbf{x}_{\mathrm{mod}_m}$ and $\dot{\mathbf{x}}_{\mathrm{mod}_m}$) should be transferred from the therapist/master site to the patient/slave site (instead of transmitting $\mathbf{x}_m$, $\dot{\mathbf{x}}_m$ and $\ddot{\mathbf{x}}_m$), as shown in Figs. 1 and 2.

Now, the nonlinear Bilateral Model Reference Adaptive Impedance Control (BMRAIC) laws for the master and slave robots are defined in Cartesian coordinates, as:

$$\begin{aligned}\mathbf{f}_m = {} & \hat{\mathbf{M}}_{\mathbf{x},m}(\mathbf{q}_m)\begin{pmatrix}-\left(m_m^{-1}c_m\right)\dot{\mathbf{x}}_m-\left(m_m^{-1}k_m\right)\left(\mathbf{x}_m-\mathbf{x}_0\right)\\+\left(m_m^{-1}\right)\left(\mathbf{f}_{th}-k_{\mathrm{f}}\mathbf{f}_{pa}\right)+\lambda_{3,m}^2\tilde{\mathbf{x}}_m\end{pmatrix}\\ & +\hat{\mathbf{C}}_{\mathbf{x},m}(\mathbf{q}_m,\dot{\mathbf{q}}_m)\dot{\mathbf{x}}_{\mathbf{r},m}+\hat{\mathbf{G}}_{\mathbf{x},m}(\mathbf{q}_m)+\hat{\mathbf{F}}_{\mathbf{x},m}(\dot{\mathbf{q}}_m)-\mathbf{f}_{th}\end{aligned} \tag{17}$$

$$\begin{aligned}\mathbf{f}_s = {} & \hat{\mathbf{M}}_{\mathbf{x},s}(\mathbf{q}_s)\begin{pmatrix}k_{\mathrm{p}}\hat{\ddot{\mathbf{x}}}_m-\left(m_s^{-1}c_s\right)\left(\dot{\mathbf{x}}_s-k_{\mathrm{p}}\dot{\mathbf{x}}_m\right)\\-\left(m_s^{-1}k_s\right)\left(\mathbf{x}_s-k_{\mathrm{p}}\mathbf{x}_m\right)\\+\left(m_s^{-1}\right)\left(-\mathbf{f}_{pa}\right)+\lambda_{3,s}^2\tilde{\mathbf{x}}_s\end{pmatrix}\\ & +\hat{\mathbf{C}}_{\mathbf{x},s}(\mathbf{q}_s,\dot{\mathbf{q}}_s)\dot{\mathbf{x}}_{\mathbf{r},s}+\hat{\mathbf{G}}_{\mathbf{x},s}(\mathbf{q}_s)+\hat{\mathbf{F}}_{\mathbf{x},s}(\dot{\mathbf{q}}_s)+\mathbf{f}_{pa}-\eta_s\,\mathrm{sgn}(\mathbf{s}_s)\end{aligned} \tag{18}$$

The accent $\hat{}$ denotes the estimation of matrices, vectors and scalars. η_s is a positive constant and it will be proved that the term $-\eta_s\,\mathrm{sgn}(\mathbf{s}_s)$ guarantees the robustness of the bilateral tele-rehabilitation system against the bounded estimation error of the master robot acceleration ($\hat{\ddot{\mathbf{x}}}_m-\ddot{\mathbf{x}}_m$). Note that the "sgn" function in the slave control law (18) may lead to undesired discontinuities and chattering in the input torques of the slave robot. Thus, the "sgn" function can be modified and replaced by continuous function alternatives (e.g., "tanh") in the experimental studies. The actual control inputs of the robots (applied in the joint space by motors) are obtained in terms of joint space matrices and vectors via employing Eq. (6) in Eqs. (17) and (18) and using Property 1 as:

$$\boldsymbol{\tau}_m = \mathbf{Y}_{\mathbf{q},m}\,\hat{\boldsymbol{\alpha}}_{\mathbf{q},m}-\mathbf{J}_m^T\mathbf{f}_{th} \tag{19}$$

$$\boldsymbol{\tau}_s = \mathbf{Y}_{\mathbf{q},s}\,\hat{\boldsymbol{\alpha}}_{\mathbf{q},s}+\mathbf{J}_s^T\mathbf{f}_{pa}-\mathbf{J}_s^T\,\eta_s\,\mathrm{sgn}(\mathbf{s}_s) \tag{20}$$

where $\mathbf{Y}_{\mathbf{q},s}$ and $\mathbf{Y}_{\mathbf{q},s}$ are obtained from Eq. (7) in terms of the following $\boldsymbol{\varphi}_{\mathbf{1},m}$, $\boldsymbol{\varphi}_{\mathbf{1},s}$, $\boldsymbol{\varphi}_{\mathbf{2},m}$, and $\boldsymbol{\varphi}_{\mathbf{2},s}$ vectors:

$$\begin{aligned}\boldsymbol{\varphi}_{\mathbf{1},m} &= \mathbf{J}_m^{-1}\begin{pmatrix}-\left(m_m^{-1}c_m\right)\dot{\mathbf{x}}_m\\-\left(m_m^{-1}k_m\right)\left(\mathbf{x}_m-\mathbf{x}_0\right)\\+\left(m_m^{-1}\right)\left(\mathbf{f}_{th}-k_{\mathrm{f}}\mathbf{f}_{pa}\right)+\lambda_{3,m}^2\tilde{\mathbf{x}}_m\end{pmatrix}-\mathbf{J}_m^{-1}\dot{\mathbf{J}}_m\mathbf{J}_m^{-1}\dot{\mathbf{x}}_{\mathbf{r},m},\\ \boldsymbol{\varphi}_{\mathbf{1},s} &= \mathbf{J}_s^{-1}\begin{pmatrix}k_{\mathrm{p}}\hat{\ddot{\mathbf{x}}}_m-\left(m_s^{-1}c_s\right)\left(\dot{\mathbf{x}}_s-k_{\mathrm{p}}\dot{\mathbf{x}}_m\right)\\-\left(m_s^{-1}k_s\right)\left(\mathbf{x}_s-k_{\mathrm{p}}\mathbf{x}_m\right)\\+\left(m_s^{-1}\right)\left(-\mathbf{f}_{pa}\right)+\lambda_{3,s}^2\tilde{\mathbf{x}}_s\end{pmatrix}-\mathbf{J}_s^{-1}\dot{\mathbf{J}}_s\mathbf{J}_s^{-1}\dot{\mathbf{x}}_{\mathbf{r},s},\\ \boldsymbol{\varphi}_{\mathbf{2},m} &= \mathbf{J}_m^{-1}\dot{\mathbf{x}}_{\mathbf{r},m}\ ,\qquad \boldsymbol{\varphi}_{\mathbf{2},s} = \mathbf{J}_s^{-1}\dot{\mathbf{x}}_{\mathbf{r},s}\end{aligned} \tag{21}$$

The closed-loop dynamics of the master and slave robots using the proposed nonlinear Bilateral Model Reference Adaptive Impedance Controller is obtained in this section. For this purpose, the control laws (17) and (18) are replaced in the nonlinear system dynamics (3) and (4) that yields:

$$\begin{aligned}&\mathbf{M}_{\mathbf{x},m}\begin{pmatrix}\ddot{\mathbf{x}}_m+\left(m_m^{-1}c_m\right)\dot{\mathbf{x}}_m+\left(m_m^{-1}k_m\right)\left(\mathbf{x}_m-\mathbf{x}_0\right)\\-\left(m_m^{-1}\right)\left(\mathbf{f}_{th}-k_{\mathrm{f}}\mathbf{f}_{pa}\right)-\lambda_{3,m}^2\tilde{\mathbf{x}}_m\end{pmatrix}=\\ &\left(\hat{\mathbf{M}}_{\mathbf{x},m}-\mathbf{M}_{\mathbf{x},m}\right)\begin{pmatrix}-\left(m_m^{-1}c_m\right)\dot{\mathbf{x}}_m-\left(m_m^{-1}k_m\right)\left(\mathbf{x}_m-\mathbf{x}_0\right)\\+\left(m_m^{-1}\right)\left(\mathbf{f}_{th}-k_{\mathrm{f}}\mathbf{f}_{pa}\right)+\lambda_{3,m}^2\tilde{\mathbf{x}}_m\end{pmatrix}\\ &+\left(\hat{\mathbf{C}}_{\mathbf{x},m}-\mathbf{C}_{\mathbf{x},m}\right)\dot{\mathbf{x}}_{\mathbf{r},m}-\mathbf{C}_{\mathbf{x},m}\mathbf{s}_m+\left(\hat{\mathbf{G}}_{\mathbf{x},m}-\mathbf{G}_{\mathbf{x},m}\right)+\left(\hat{\mathbf{F}}_{\mathbf{x},m}-\mathbf{F}_{\mathbf{x},m}\right)\end{aligned} \tag{22}$$

$$\begin{aligned}&\mathbf{M}_{\mathbf{x},s}\begin{pmatrix}\left(\ddot{\mathbf{x}}_s-k_{\mathrm{p}}\ddot{\mathbf{x}}_m\right)+\left(m_s^{-1}c_s\right)\left(\dot{\mathbf{x}}_s-k_{\mathrm{p}}\dot{\mathbf{x}}_m\right)\\+\left(m_s^{-1}k_s\right)\left(\mathbf{x}_s-k_{\mathrm{p}}\mathbf{x}_m\right)-\left(m_s^{-1}\right)\left(-\mathbf{f}_{pa}\right)-\lambda_{3,s}^2\tilde{\mathbf{x}}_s\end{pmatrix}=\\ &\quad+\mathbf{M}_{\mathbf{x},s}k_{\mathrm{p}}\left(\hat{\ddot{\mathbf{x}}}_m-\ddot{\mathbf{x}}_m\right)\\ &\quad+\left(\hat{\mathbf{M}}_{\mathbf{x},s}-\mathbf{M}_{\mathbf{x},s}\right)\begin{pmatrix}k_{\mathrm{p}}\hat{\ddot{\mathbf{x}}}_m-\left(m_s^{-1}c_s\right)\left(\dot{\mathbf{x}}_s-k_{\mathrm{p}}\dot{\mathbf{x}}_m\right)\\-\left(m_s^{-1}k_s\right)\left(\mathbf{x}_s-k_{\mathrm{p}}\mathbf{x}_m\right)\\+\left(m_s^{-1}\right)\left(-\mathbf{f}_{pa}\right)+\lambda_{3,s}^2\tilde{\mathbf{x}}_s\end{pmatrix}\\ &\quad+\left(\hat{\mathbf{C}}_{\mathbf{x},s}-\mathbf{C}_{\mathbf{x},s}\right)\dot{\mathbf{x}}_{\mathbf{r},s}-\mathbf{C}_{\mathbf{x},s}\mathbf{s}_s+\left(\hat{\mathbf{G}}_{\mathbf{x},s}-\mathbf{G}_{\mathbf{x},s}\right)\\ &\quad+\left(\hat{\mathbf{F}}_{\mathbf{x},s}-\mathbf{F}_{\mathbf{x},s}\right)-\eta_s\,\mathrm{sgn}(\mathbf{s}_s)\end{aligned} \tag{23}$$

where the first term in the left side of Eq. (23) is obtained as:

$$\left(\ddot{\mathbf{x}}_s - k_{\mathrm{p}}\ddot{\mathbf{x}}_m\right) = \left(\ddot{\mathbf{x}}_s - k_{\mathrm{p}}\hat{\ddot{\mathbf{x}}}_m\right) - k_{\mathrm{p}}\left(\ddot{\mathbf{x}}_m - \hat{\ddot{\mathbf{x}}}_m\right) \tag{24}$$

Then, the master reference model (9) is multiplied by $\mathbf{M}_{\mathbf{x},m}m_m^{-1}$ and subtracted from Eq. (22), and the slave reference model (10) is multiplied by $\mathbf{M}_{\mathbf{x},s}m_s^{-1}$ and subtracted from Eq. (23), and based on Property 1 and using Eqs. (7) and (21), we have:

$$\begin{aligned}\mathbf{M}_{\mathbf{x},m}\left(\dddot{\tilde{\mathbf{x}}}_m + \left(m_m^{-1}c_m\right)\ddot{\tilde{\mathbf{x}}}_m + \left(m_m^{-1}k_m\right)\dot{\tilde{\mathbf{x}}}_m - \lambda_{3,m}^2\tilde{\mathbf{x}}_m\right) = \\ -\mathbf{C}_{\mathbf{x},m}\mathbf{s}_m + \mathbf{J}_m^{-T}\mathbf{Y}_{\mathbf{q},m}\tilde{\boldsymbol{\alpha}}_{\mathbf{q},m}\end{aligned} \tag{25}$$

$$\begin{aligned}\mathbf{M}_{\mathbf{x},s}\left(\dddot{\tilde{\mathbf{x}}}_s + \left(m_s^{-1}c_s\right)\ddot{\tilde{\mathbf{x}}}_s + \left(m_s^{-1}k_s\right)\dot{\tilde{\mathbf{x}}}_s - \lambda_{3,s}^2\tilde{\mathbf{x}}_s\right) = \\ -\mathbf{C}_{\mathbf{x},s}\mathbf{s}_s + \mathbf{J}_s^{-T}\mathbf{Y}_{\mathbf{q},s}\tilde{\boldsymbol{\alpha}}_{\mathbf{q},s} \\ + \mathbf{M}_{\mathbf{x},s}k_{\mathrm{p}}\left(\hat{\ddot{\mathbf{x}}}_m - \ddot{\mathbf{x}}_m\right) - \eta_s\,\mathrm{sgn}(\mathbf{s}_s)\end{aligned} \tag{26}$$

where $\tilde{\boldsymbol{\alpha}}_{\mathbf{q},m} = \hat{\boldsymbol{\alpha}}_{\mathbf{q},m} - \boldsymbol{\alpha}_{\mathbf{q},m}$ and $\tilde{\boldsymbol{\alpha}}_{\mathbf{q},s} = \hat{\boldsymbol{\alpha}}_{\mathbf{q},s} - \boldsymbol{\alpha}_{\mathbf{q},s}$ are the error vectors of the master and slave parameter estimations, respectively. Substituting Eq. (14) in the left side of Eqs. (25) and (26) resulted in:

$$\mathbf{M}_{\mathbf{x},m}\left(\left((d/dt) + \lambda_{2,m}\right)\mathbf{s}_m\right) = -\mathbf{C}_{\mathbf{x},m}\mathbf{s}_m + \mathbf{J}_m^{-T}\mathbf{Y}_{\mathbf{q},m}\tilde{\boldsymbol{\alpha}}_{\mathbf{q},m} \tag{27}$$

$$\begin{aligned}\mathbf{M}_{\mathbf{x},s}\left(\left((d/dt) + \lambda_{2,s}\right)\mathbf{s}_s\right) = -\mathbf{C}_{\mathbf{x},s}\mathbf{s}_s + \mathbf{J}_s^{-T}\mathbf{Y}_{\mathbf{q},s}\tilde{\boldsymbol{\alpha}}_{\mathbf{q},s} \\ + \mathbf{M}_{\mathbf{x},s}k_{\mathrm{p}}\left(\hat{\ddot{\mathbf{x}}}_m - \ddot{\mathbf{x}}_m\right) - \eta_s\,\mathrm{sgn}(\mathbf{s}_s)\end{aligned} \tag{28}$$

Finally, the closed-loop dynamics of the nonlinear tele-rehabilitation system is obtained from (27) and (28) as:

$$\mathbf{M}_{\mathbf{x},m}\dot{\mathbf{s}}_m = -\lambda_{2,m}\mathbf{M}_{\mathbf{x},m}\mathbf{s}_m - \mathbf{C}_{\mathbf{x},m}\mathbf{s}_m + \mathbf{J}_m^{-T}\mathbf{Y}_{\mathbf{q},m}\tilde{\boldsymbol{\alpha}}_{\mathbf{q},m} \tag{29}$$

$$\begin{aligned}\mathbf{M}_{\mathbf{x},s}\dot{\mathbf{s}}_s = -\lambda_{2,s}\mathbf{M}_{\mathbf{x},s}\mathbf{s}_s - \mathbf{C}_{\mathbf{x},s}\mathbf{s}_s + \mathbf{J}_s^{-T}\mathbf{Y}_{\mathbf{q},s}\tilde{\boldsymbol{\alpha}}_{\mathbf{q},s} \\ + \mathbf{M}_{\mathbf{x},s}k_{\mathrm{p}}\left(\hat{\ddot{\mathbf{x}}}_m - \ddot{\mathbf{x}}_m\right) - \eta_s\,\mathrm{sgn}(\mathbf{s}_s)\end{aligned} \tag{30}$$

As seen, due to the MRAIC structure of the proposed controller, the real parts ($\lambda_{1,i}$ and $\lambda_{2,i}$) of the stable poles of the reference impedance models (introduced in Eq. (11)) facilitate the design of the proposed controller. Indeed, one set of these positive parameters ($\lambda_{1,m}$ and $\lambda_{1,s}$) guarantees the stability of the sliding surfaces $\mathbf{s}_m$ and $\mathbf{s}_s$ in (13). Also, the other set of the stable poles' parameters ($\lambda_{2,m}$ and $\lambda_{2,s}$) guarantees the stability of the closed-loop dynamics of the tele-rehabilitation system in Eqs. (29) and (30), which will be proved in the next section. Therefore, the stability features of the impedance models (9) and (10) are employed in the design of the proposed nonlinear bilateral controller.

5. Lyapunov Stability Proof and Adaptation Laws

In this section, the stability of the proposed bilateral tele-rehabilitation system in the presence of parametric modeling uncertainties and bounded estimation error of the master robot acceleration is studied. Also, the tracking convergence of the master and slave trajectories ($\mathbf{x}_m$ and $\mathbf{x}_s$) to the desired impedance model responses ($\mathbf{x}_{\mathrm{mod}_m}$ and $\mathbf{x}_{\mathrm{mod}_s}$) is proved. To this end, a positive definite Lyapunov function is defined as:

$$\begin{aligned}V(t) = \frac{1}{2}\Big(&\mathbf{s}_m^T\mathbf{M}_{\mathbf{x},m}\mathbf{s}_m + \mathbf{s}_s^T\mathbf{M}_{\mathbf{x},s}\mathbf{s}_s \\ &+ \tilde{\boldsymbol{\alpha}}_{\mathbf{q},m}^T\boldsymbol{\Gamma}_m^{-1}\tilde{\boldsymbol{\alpha}}_{\mathbf{q},m} + \tilde{\boldsymbol{\alpha}}_{\mathbf{q},s}^T\boldsymbol{\Gamma}_s^{-1}\tilde{\boldsymbol{\alpha}}_{\mathbf{q},s}\Big)\end{aligned} \tag{31}$$

where $\boldsymbol{\Gamma}_m$ and $\boldsymbol{\Gamma}_s$ are symmetric positive definite matrices named adaptation gains. It should be noted that the first two terms of the Lyapunov function (including $\mathbf{s}_m$ and $\mathbf{s}_s$) are defined in Cartesian coordinates; however, the last two terms (in terms of $\tilde{\boldsymbol{\alpha}}_{\mathbf{q},m}$ and $\tilde{\boldsymbol{\alpha}}_{\mathbf{q},s}$) originated from the joint space parameterization. The time derivative of Lyapuniv function V is obtained as:

$$\begin{aligned}\dot{V}(t) = &\mathbf{s}_m^T\left(\mathbf{M}_{\mathbf{x},m}\dot{\mathbf{s}}_m + \frac{1}{2}\dot{\mathbf{M}}_{\mathbf{x},m}\mathbf{s}_m\right) \\ &+ \mathbf{s}_s^T\left(\mathbf{M}_{\mathbf{x},s}\dot{\mathbf{s}}_s + \frac{1}{2}\dot{\mathbf{M}}_{\mathbf{x},s}\mathbf{s}_s\right) + \dot{\tilde{\boldsymbol{\alpha}}}_{\mathbf{q},m}^T\boldsymbol{\Gamma}_m^{-1}\tilde{\boldsymbol{\alpha}}_{\mathbf{q},m} + \dot{\tilde{\boldsymbol{\alpha}}}_{\mathbf{q},s}^T\boldsymbol{\Gamma}_s^{-1}\tilde{\boldsymbol{\alpha}}_{\mathbf{q},s}\end{aligned} \tag{32}$$

where $\dot{\tilde{\boldsymbol{\alpha}}}_{\mathbf{q},i} = \dot{\hat{\boldsymbol{\alpha}}}_{\mathbf{q},i}$ because $\tilde{\boldsymbol{\alpha}}_{\mathbf{q},i} = \hat{\boldsymbol{\alpha}}_{\mathbf{q},i} - \boldsymbol{\alpha}_{\mathbf{q},i}$ and $\boldsymbol{\alpha}_{\mathbf{q},i}$ is the constant vector of the actual parameters ($\dot{\boldsymbol{\alpha}}_{\mathbf{q},i} = 0$). Substituting the final closed-loop dynamics of the nonlinear tele-rehabilitation system (Eqs. (29) and (30)) in Eq. (32), $\dot{V}(t)$ is found as:

$$\begin{aligned}\dot{V}(t) = & -\lambda_{2,m}\mathbf{s}_m^T\mathbf{M}_{\mathbf{x},m}\mathbf{s}_m - \lambda_{2,s}\mathbf{s}_s^T\mathbf{M}_{\mathbf{x},s}\mathbf{s}_s \\ & + \frac{1}{2}\mathbf{s}_m^T\left(\dot{\mathbf{M}}_{\mathbf{x},m} - 2\mathbf{C}_{\mathbf{x},m}\right)\mathbf{s}_m + \frac{1}{2}\mathbf{s}_s^T\left(\dot{\mathbf{M}}_{\mathbf{x},s} - 2\mathbf{C}_{\mathbf{x},s}\right)\mathbf{s}_s \\ & + \mathbf{s}_m^T\mathbf{J}_m^{-T}\mathbf{Y}_{\mathbf{q},m}\tilde{\boldsymbol{\alpha}}_{\mathbf{q},m} + \mathbf{s}_s^T\mathbf{J}_m^{-T}\mathbf{Y}_{\mathbf{q},s}\tilde{\boldsymbol{\alpha}}_{\mathbf{q},s} \\ & + \mathbf{s}_s^T\left(\mathbf{M}_{\mathbf{x},s}k_{\mathrm{p}}\left(\hat{\ddot{\mathbf{x}}}_m - \ddot{\mathbf{x}}_m\right) - \eta_s\,\mathrm{sgn}(\mathbf{s}_s)\right) \\ & + \dot{\hat{\boldsymbol{\alpha}}}_{\mathbf{q},m}^T\boldsymbol{\Gamma}_m^{-1}\tilde{\boldsymbol{\alpha}}_{\mathbf{q},m} + \dot{\hat{\boldsymbol{\alpha}}}_{\mathbf{q},s}^T\boldsymbol{\Gamma}_s^{-1}\tilde{\boldsymbol{\alpha}}_{\mathbf{q},s}\end{aligned} \tag{33}$$

Now, the adaptation laws for the estimation of the vector of unknown parameters in the master and slave dynamic models are defined as:

$$\dot{\hat{\boldsymbol{\alpha}}}_{\mathbf{q},m} = -\boldsymbol{\Gamma}_m^T\mathbf{Y}_{\mathbf{q},m}^T\mathbf{J}_m^{-1}\mathbf{s}_m\ ,\quad \dot{\hat{\boldsymbol{\alpha}}}_{\mathbf{q},s} = -\boldsymbol{\Gamma}_s^T\mathbf{Y}_{\mathbf{q},s}^T\mathbf{J}_s^{-1}\mathbf{s}_s \tag{34}$$

For implementing the proposed control laws (19) and (20) as the motor torques and the proposed adaptation laws (34) in the joint space, the non-singularity of Jacobian matrices $\mathbf{J}_m$ and $\mathbf{J}_s$ is necessary, as mentioned for Eq. (6). Substituting the adaptation laws (34) in the time derivative of the Lyapunov function, and using Property 2 of the robot dynamics ($\dot{\mathbf{M}}_{\mathbf{x},i} - 2\mathbf{C}_{\mathbf{x},i}$ is skew symmetric), Eq. (33) reduces to:

$$\begin{aligned}\dot{V}(t) = & -\lambda_{2,m}\mathbf{s}_m^T\mathbf{M}_{\mathbf{x},m}\mathbf{s}_m - \lambda_{2,s}\mathbf{s}_s^T\mathbf{M}_{\mathbf{x},s}\mathbf{s}_s \\ & + \mathbf{s}_s^T\left(\mathbf{M}_{\mathbf{x},s}k_{\mathrm{p}}\left(\hat{\ddot{\mathbf{x}}}_m - \ddot{\mathbf{x}}_m\right) - \eta_s\,\mathrm{sgn}(\mathbf{s}_s)\right)\end{aligned} \tag{35}$$

Note that $\dot{\mathbf{x}}_{\mathrm{mod}_m}$ and $\mathbf{x}_{\mathrm{mod}_m}$ are bounded as the response of the stable master impedance model (9) with bounded inputs (bounded interaction forces $\mathbf{f}_{th}$ and $\mathbf{f}_{pa}$), which implies the boundedness of $\hat{\ddot{\mathbf{x}}}_m$ obtained from (16). Moreover, it is reasonable that the master acceleration $\ddot{\mathbf{x}}_m$ is bounded because the master robot (3) is a physical system (with a second-order differential equation) having bounded input forces $\mathbf{f}_{th}$ and $\mathbf{f}_m$. Therefore, the estimation error of the master robot acceleration ($\hat{\ddot{\mathbf{x}}}_m - \ddot{\mathbf{x}}_m$) in Eq. (35) is bounded. In order to guarantee the robustness against this bounded error, the positive constant parameter η_s in the slave control law (18) should satisfy the following component-wise inequality:

$$\eta_s \geq \left\|\mathbf{M}_{\mathbf{x},s}k_{\mathrm{p}}\left(\hat{\ddot{\mathbf{x}}}_m - \ddot{\mathbf{x}}_m\right)\right\|_\infty + \varepsilon_s \tag{36}$$

where ε_s is a positive constant. It should be mentioned that the actual parameters in $\mathbf{M}_{\mathbf{x},s}$ are uncertain in this adaptive control strategy. Moreover, the bounded error of the acceleration estimation ($\hat{\ddot{\mathbf{x}}}_m - \ddot{\mathbf{x}}_m$) is unknown. However, to have the stability property, η_s should be larger than the maximum value of $\left\|\mathbf{M}_{\mathbf{x},s}k_{\mathrm{p}}(\hat{\ddot{\mathbf{x}}}_m - \ddot{\mathbf{x}}_m)\right\|_\infty$, due to Eq. (36). In other words, η_s should be chosen as large (using a trial and error practical method) that the stability of the system against bounded acceleration estimation error is ensured; which means the inequality (36) is satisfied. As a result, the time derivative of the Lyapunov function (35) becomes:

$$\dot{V}(t) \leq -\lambda_{2,m}\mathbf{s}_m^T\mathbf{M}_{\mathbf{x},m}\mathbf{s}_m - \lambda_{2,s}\mathbf{s}_s^T\mathbf{M}_{\mathbf{x},s}\mathbf{s}_s - \varepsilon_s\left\|\mathbf{s}_s\right\|_1 \tag{37}$$

Theorem. *Based on the positive definiteness of inertia matrices* $\mathbf{M}_{\mathbf{x},m}$, $\mathbf{M}_{\mathbf{x},s}$ *(Property 3) and adaptation gain matrices* $\boldsymbol{\Gamma}_m$ *and* $\boldsymbol{\Gamma}_s$, *the Lyapunov function (31) is positive definite* ($V(t) \geq 0$) *and its time derivative (37) is negative definite* ($\dot{V}(t) \leq 0$). *Under this condition, the tracking convergence to sliding surfaces* $\mathbf{s}_m = 0$ *and* $\mathbf{s}_s = 0$, *and the boundedness of* $\tilde{\boldsymbol{\alpha}}_{\mathbf{q},m}$ *and* $\tilde{\boldsymbol{\alpha}}_{\mathbf{q},s}$ *are concluded.*

Proof. According to the Barbalat's lemma [44], if w is a uniformly continuous function for $t \geq 0$ and if the limit of the integral $\lim_{t\to\infty}\int_0^t w(\zeta)\,d\zeta$ exists and has a finite value; then, it is concluded that: $\lim_{t\to\infty} w(t) = 0$.

Now, assuming $w(t) = \lambda_{2,m}\mathbf{s}_m^T\mathbf{M}_{\mathbf{x},m}\mathbf{s}_m + \lambda_{2,s}\mathbf{s}_s^T\mathbf{M}_{\mathbf{x},s}\mathbf{s}_s + \varepsilon_s\left\|\mathbf{s}_s\right\|_1 \geq 0$ as a uniformly continuous function, and then by integrating Eq. (37) over time, it is obtained that:

$$V(0) - V(\infty) \geq \lim_{t\to\infty}\int_0^t w(\zeta)\,d\zeta \tag{38}$$

Moreover, since $\dot{V}(t) = dV(t)/dt \leq 0$ is negative due to Eq. (37), $V(0) - V(\infty) \geq 0$ is positive and finite. As a result,

$\lim_{t\to\infty}\int_0^t w(\zeta)\,d\zeta$ in Eq. (38) has a finite and positive value (based on the positiveness of $w(t)$). Therefore, according to the Barbalat's lemma [44], one can write:

$$\lim_{t\to\infty} w(t) = \lim_{t\to\infty}\left(\lambda_{2,m}\mathbf{s}_m^T\mathbf{M}_{\mathbf{x},m}\mathbf{s}_m + \lambda_{2,s}\mathbf{s}_s^T\mathbf{M}_{\mathbf{x},s}\mathbf{s}_s + \varepsilon_s\left\|\mathbf{s}_s\right\|_1\right) = 0 \quad (39)$$

Since $\lambda_{2,m}$, $\lambda_{2,s}$ and ε_s are positive (nonzero) constants, and regarding $\mathbf{s}_m^T\mathbf{M}_{\mathbf{x},m}\mathbf{s}_m \geq 0$, $\mathbf{s}_s^T\mathbf{M}_{\mathbf{x},s}\mathbf{s}_s \geq 0$ and $\left\|\mathbf{s}_s\right\|_1 \geq 0$, Eq. (39) implies the convergence to sliding surfaces $\mathbf{s}_m = 0$ and $\mathbf{s}_s = 0$ as $t \to \infty$. The positiveness of $V(t) \geq 0$ and negativeness of $\dot{V}(t) \leq 0$ also imply that the Lyapunov function (31) is bounded. Therefore, due to the convergence of $\mathbf{s}_m \to 0$ and $\mathbf{s}_s \to 0$ and the boundedness of $V(t)$, Eq. (31) ensures that the parameter estimation errors $\tilde{\boldsymbol{\alpha}}_{\mathbf{q},m}$ and $\tilde{\boldsymbol{\alpha}}_{\mathbf{q},s}$ will remain bounded.

Since the dynamics of the master and slave sliding surfaces $\mathbf{s}_m = 0$ and $\mathbf{s}_s = 0$ are stable ($\lambda_{1,m}$ and $\lambda_{1,s}$ in Eq. (13) are positive), it is proved that the tracking errors converge to zero ($\tilde{\mathbf{x}}_m \to 0$ and $\tilde{\mathbf{x}}_s \to 0$) on the surfaces of $\mathbf{s}_m = 0$ and $\mathbf{s}_s = 0$. Consequently, the master and slave robots track and realize their corresponding reference impedance models ($\mathbf{x}_m \to \mathbf{x}_{\mathrm{mod}_m}$ and $\mathbf{x}_s \to \mathbf{x}_{\mathrm{mod}_s}$), which is the objective of the proposed bilateral controller.

5.1. Safety of the robotic tele-rehabilitation system

As mentioned before, the stability of the master and slave impedance models (9) and (10) with positive impedance parameters implies that the bounded forces of the patient ($\mathbf{f}_{pa}$) and therapist ($\mathbf{f}_{th}$) will generate bounded desired trajectories for the master ($\mathbf{x}_{\mathrm{mod}_m}$) and slave ($\mathbf{x}_{\mathrm{mod}_s}$) robots. In addition, the above Lyapunov stability proof guarantees the boundedness of tracking errors ($\mathbf{s}_m$ and $\mathbf{s}_s$) and their convergence to zero ($\mathbf{s}_m \to 0$ and $\mathbf{s}_s \to 0$ that results $\mathbf{x}_m \to \mathbf{x}_{\mathrm{mod}_m}$ and $\mathbf{x}_s \to \mathbf{x}_{\mathrm{mod}_s}$) using the proposed nonlinear bilateral adaptive controller. Based on the combination of impedance models' stability and the Lyapunov-based stability of the closed-loop nonlinear dynamics of tele-rehabilitation system, the bounded input forces of the patient ($\mathbf{f}_{pa}$) and the therapist ($\mathbf{f}_{th}$) will result in bounded trajectories for master ($\mathbf{x}_m$) and slave ($\mathbf{x}_s$) robots. This implies the absolute stability of the proposed nonlinear multi-DOF tele-rehabilitation system. The stability characteristic of the proposed method guarantees the safety of the patient and therapist during their interactions with robot manipulators, which is an important issue in robotic tele-rehabilitation systems [8].

6. Experimental Evaluations of Tele-Rehabilitation Modes

In this section, the proposed bilateral impedance control framework is evaluated through experiments on a multi-DOF tele-robotic system. In this system, a 3-DOF Phantom Premium 1.5A robot (Geomagic Inc., Wilmington, MA), which is a light-weight haptic device, is used as the master robot (Fig. 3). Also, a 2-DOF planar Quanser Rehab Robot (Quanser Consulting Inc., Markham, ON) designed for the upper limb is employed as the slave robot (Fig. 3). The Quanser Rehab and Phantom Premium robots are equipped with an ATI Gamma force/torque sensor (ATI Industrial Automation, Apex, NC) and a JR3 50M31 force/torque sensor (JR3 Inc., Woodland, CA), respectively, to measure the applied interaction forces of the patient and the therapist along Cartesian axes. Using a UDP-based communication channel, the force and position data is transmitted between the master and the slave robots. Employing the QUARC (Quanser Real-Time Control) software, the proposed bilateral impedance controller is implemented with a sampling rate of $1\ k\mathrm{Hz}$.

An interactive reaching task is developed where a dynamic moving target is shown (Fig. 3) for two able-bodied users acting as the therapist and the patient. Each of the therapist and the patient has a monitor to observe both robots positions in the $x-y$ plane with respect to the target point. The

positions of the patient, the therapist and the target point are shown with the blue circle, red square and yellow circle, respectively, in both screens. These positions are plotted with the same sampling rate ($1\,k$Hz) as the controller using the real-time software (QUARC). The plots have been generated using the two-dimensional "XY Figure block" of QUARC.

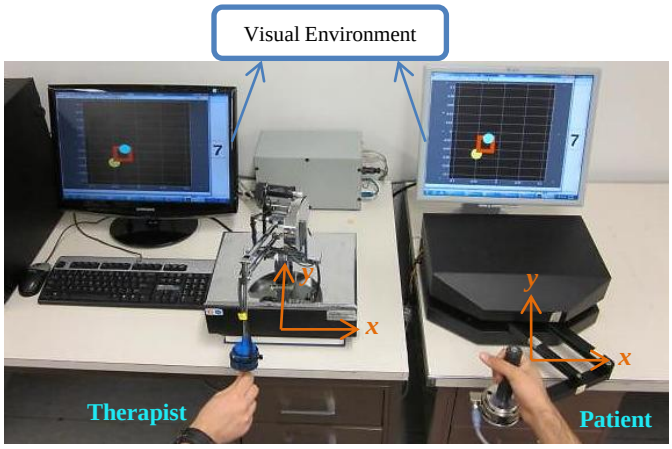

Fig. 3. The experimental tele-rehabilitation set-up: the master is Phantom Premium robot (left) and the slave is Quanser Rehab robot (right).

In this paper, the goal is mainly to evaluate the performance of the proposed bilateral impedance controller in terms of facilitating different tele-rehabilitation modes and therefore a healthy person behaves as the patient in these experiments. However, more user studies involving patients (outside the scope of this paper) will need to be performed in the future.

The workspace of the slave robot is a subset of the horizontal $x-y$ plane shown in Fig. 3. Also, the master robot is controlled to have motions in the same two dimensional $x-y$ plane. Thus, the Cartesian position of robots' end-effector is defined as $\mathbf{x}_i = [x \quad y]_i^T$ ($i = m, s$). The kinematics and dynamics of the Phantom Premium (master) and Quanser Rehab (slave) robots were presented in [47] and [48, 49], respectively. Moreover, the operating workspace in these experiments is designed to be far from the singular positions of the master and slave robots in order to have nonsingular Jacobian matrices ($\mathbf{J}_m$ and $\mathbf{J}_s$).

The parameters of the impedance models for the master (9) and the slave (10) are designed for two tele-rehabilitation modes as discussed in Sec. 3 and summarized in Table 1. Accordingly, in these experiments, the stiffness value in each impedance model (k_m and/or k_s) is selected based on the desired relationship between the forces and positions in each mode (see Table 1). The damping ratio of the impedance models (9) and (10) is also selected as $\zeta_i = c_i / 2\sqrt{m_i k_i} = 0.7$ such that they have a fast response with respect to the dimensionless time $\omega_{n_i} t$ (with appropriate overshoot value in response to the step forces). After that, the natural frequency (which is the cut-off frequency when $\zeta_i = 0.7$) of each impedance model is adjusted on a small value $\omega_{n_i} = \sqrt{k_i / m_i} = 2$ rad/sec such that possible hand tremors of the patient are filtered out. The position scaling factor is considered to be $k_{\mathrm{p}} = 1$ based on the approximate workspace ratio of the Phantom robot (master) and the rehab robot (slave) in the $x-y$ plane. The force scaling factor k_{f} is selected to be $k_{\mathrm{f}} = 1/3$ in order to enlarge the authority of therapist force in comparison with the patient one according to (9) as discussed in Sec. 3.1. Consequently, the employed impedance parameters and scaling factors for "hand-over-hand" and "adjustable-flexibility" cooperative tasks are listed in Table 2.

Table 2. Employed values of impedance parameters and scaling factors for cooperative tele-rehabilitation modes

Cooperative Tele-Rehab. Mode	Master Imp. Model Parameters	Slave Imp. Model Parameters	Scaling Factors
Hand-Over-Hand	$k_m = 3$ N/m $c_m = 2.1$ N.s/m $m_m = 0.75$ kg	$k_s = 5000$ N/m $c_s = 3500$ N.s/m $m_s = 1250$ kg	$k_{\mathrm{f}} = 1/3$ $k_{\mathrm{p}} = 1$
Adjustable-Flexibility	$k_m = 3$ N/m $c_m = 2.1$ N.s/m $m_m = 0.75$ kg	$k_s = 100$ N/m $c_s = 70$ N.s/m $m_s = 25$ kg	$k_{\mathrm{f}} = 1/3$ $k_{\mathrm{p}} = 1$

The other parameters used in the control laws (17) and (18) and adaptation laws (34) for these experiments are $\eta_s = 2.1$, $\mathbf{\Gamma}_m = 20\,I$ and $\mathbf{\Gamma}_s = 33\,I$. The gain η_s of the slave controller is adjusted as large as needed using a trial and error method and some initial experiments such that the teleoperation system's stability and the master and slave tracking convergence to

their desired impedance responses are achieved appropriately by satisfying inequality (36). It should be noted that the "sgn" function in the slave control law (18) may lead to undesired discontinuities and chattering in the input torques of the slave robot. Therefore, the continuous function $\tanh(120\mathbf{s}_s)$ is used as an alternative to "sgn" in our experimental studies.

In these experiments, the initial position, velocity and accelerations of the master and slave robots are zero, i.e., the robots motions start form their resting configurations. Moreover, the desired trajectories for the master ($\mathbf{x}_{\mathrm{mod}_m}$) and the slave ($\mathbf{x}_{\mathrm{mod}_s}$) obtained from the impedance models (9) and (10) have zero initial position, velocity and acceleration. Accordingly, the master and slave robots errors with respect to their desired impedance responses are initially zero ($\tilde{\mathbf{x}}_m(t_0) = \dot{\tilde{\mathbf{x}}}_m(t_0) = \ddot{\tilde{\mathbf{x}}}_m(t_0) = 0_{2\times1}$, $\tilde{\mathbf{x}}_s(t_0) = \dot{\tilde{\mathbf{x}}}_s(t_0) = \ddot{\tilde{\mathbf{x}}}_s(t_0) = 0_{2\times1}$). Consequently, the distances of the master and slave robots trajectory to their corresponding sliding surfaces (13) are zero at the initial time t_0 ($\mathbf{s}_m(t_0) = 0_{2\times1}$ and $\mathbf{s}_s(t_0) = 0_{2\times1}$). Therefore, at the initial moment, the robots trajectories are on the impedance models' responses; however after a while, the tracking errors will increase due to the robots uncertainties and applied forces of the therapist and the patient. Finally, the master and slave errors will converge to zero ($\mathbf{s}_m \to 0$ and $\mathbf{s}_s \to 0$) based on the Lyapunov stability analysis (Sec. 5) of the proposed controller.

For the cooperative tele-rehabilitation strategies, a reaching task with a moving target point is demonstrated visually on the therapist and patient monitors. The target has a circular path in the $x-y$ plane and its velocity is dynamically varying during the task. The velocity of this moving target is designed as

$$V_{\mathrm{target}}(t) = V_{\min} + \Delta V_{\mathrm{var}}(t) \tag{40}$$

where $V_{\mathrm{target}}(t)$, $V_{\min}$ and $\Delta V_{\mathrm{var}}(t)$ are the total velocity, the minimum constant velocity and the time-varying component of the velocity of the moving target. The dynamics of the time varying portion of the target velocity is defined in terms of the patient position distance with respect to the target point as:

$$\Delta\dot{V}_{\mathrm{var}} + \beta\Delta V_{\mathrm{var}} = \frac{\mu}{\delta_0 + \left\|\tilde{\mathbf{x}}_{p-t}\right\|_2} \tag{41}$$

where β, μ and δ_0 are positive constants, and $\tilde{\mathbf{x}}_{p-t}$ is the distance between the patient and target. Since the target position ($\mathbf{x}_{\mathrm{target}}$) is obtained from the integration of the target velocity (V_{target} in (40)), Eq. (41) can be solved using the numerical integration with respect to time in order to obtain ΔV_{var}. In other words, there is a delay of 1 sampling time between $\tilde{\mathbf{x}}_{p\text{-}t} = \mathbf{x}_p - \mathbf{x}_{\mathrm{target}} = \mathbf{x}_s - \mathbf{x}_{\mathrm{target}}$ in the right side of Eq. (41) and the obtained ΔV_{var} from the left side of Eq. (41). Then, the obtained ΔV_{var} is added to $V_{\min}$ based on (40) to find the total target velocity for the next sampling time.

Due to (41), the time varying portion of the target velocity ΔV_{var} increases as the distance of the patient position with respect to the target decreases (i.e., when the success of the patient in tracking the target increases). The increase in the target velocity is not sudden and has a dynamics based on (41) in which the parameter β denotes the rate of this velocity increase with respect to the time. The parameters μ and δ_0 specify the magnitude of the varying velocity ΔV_{var} with respect to the patient distance $\left\|\tilde{\mathbf{x}}_{p-t}\right\|_2$. Accordingly, the maximum varying velocity is $\Delta V_{\mathrm{var}} = \mu/\beta\delta_0$ when the patient can remain on the moving target $\left\|\tilde{\mathbf{x}}_{p-t}\right\|_2 = 0$. The parameters used for the moving target velocity dynamics (defined by (40) and (41)) are listed in Table 3.

Table 3. Parameters of the moving target velocity

Minimum Constant Velocity	Time-Varying Velocity
$V_{\min} = 0.035\ m/\sec$	$\beta = 1.5$ $\mu = 0.0004$ $\delta_0 = 0.0002$

An image of the planar visual environment provided for the therapist and patient via their monitors during the cooperation tasks is shown in Fig. 4.

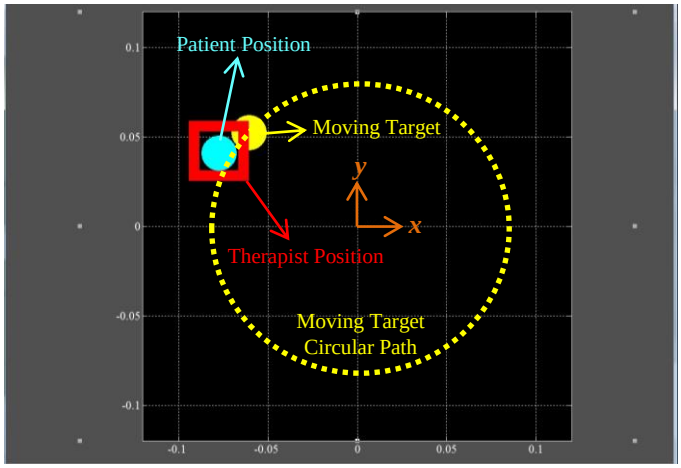

Fig. 4. The 2D visual environment provided to both the therapist and the patient during the cooperation tasks (some notes about the patient, therapist and moving target positions are added).

6.1. "Hand-Over-Hand" Cooperative Tele-rehabilitation Task

For the "hand-over-hand" cooperative tele-rehabilitation, the master impedance parameters (Table 2) are considered to be small such that the therapist and patient can move the master and slave robots easily (with small forces $\mathbf{f}_{th}$ and $\mathbf{f}_{pa}$) as shown in Fig. 5. It is also observed that the perfect force reflection is approximately achieved ($\mathbf{f}_{th} - k_f \mathbf{f}_{pa} \to 0$) as a consequence of choosing small parameters for the master impedance model (9). The slave impedance parameters for this tele-rehabilitation mode are chosen so large (see Table 2) that the patient and the therapist have the same position during the task as seen in Fig. 6.

Note that the experimental data saved in the QUARC software is employed in MATLAB for plotting different figures.

The position of robots' end-effectors together with the position response of the master and slave impedance models and the moving target in x and y directions are shown in Fig. 6. Moreover, the trajectories of the therapist, the patient, and the master and slave impedance model responses with respect to the circular trajectory of the moving target are shown in the $x-y$ plane in Fig. 7.

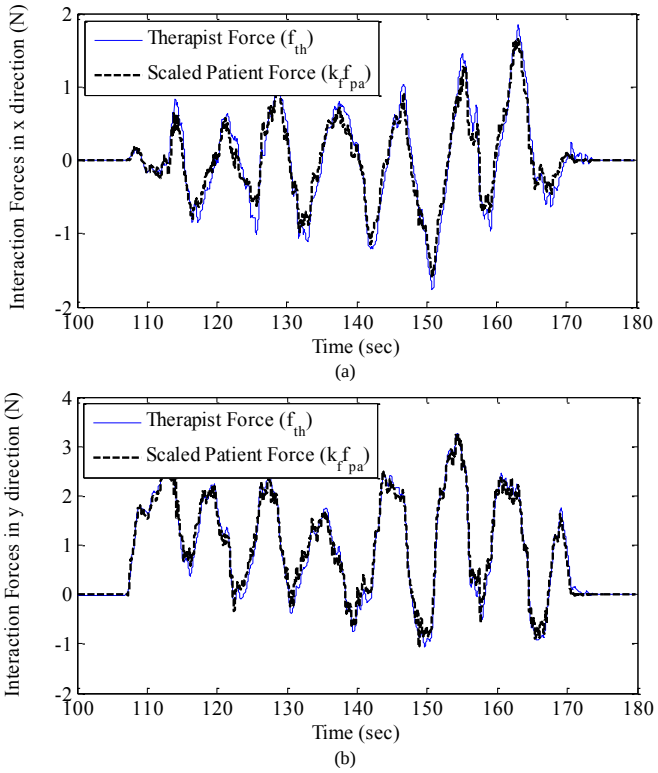

Fig. 5. The therapist force $\mathbf{f}_{th}$ and the scaled patient force $k_f \mathbf{f}_{pa}$ in (a) x and (b) y directions during the "hand-over-hand" cooperative tele-rehabilitation mode.

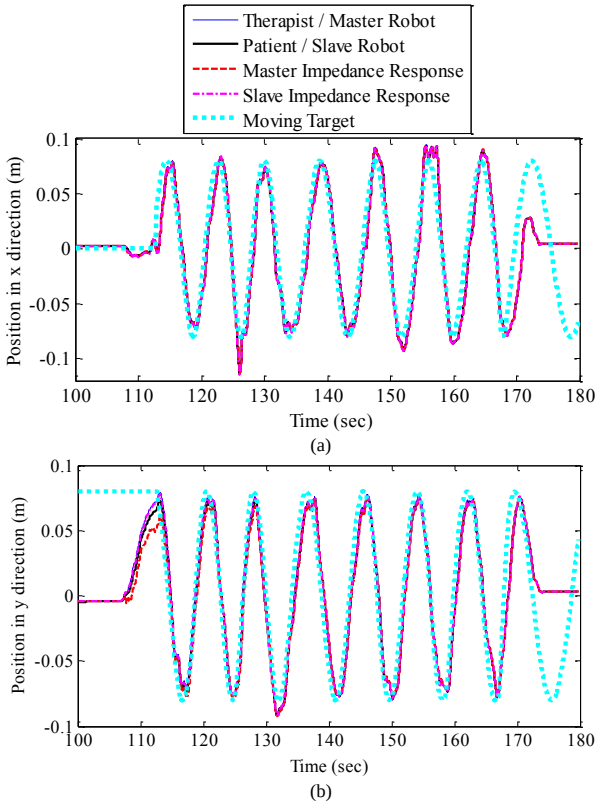

Fig. 6. The positions of the therapist's and the patient's hands together with the corresponding master and slave impedance models responses in (a) x and (b) y directions, for the "hand-over-hand" cooperative tele-rehabilitation mode.

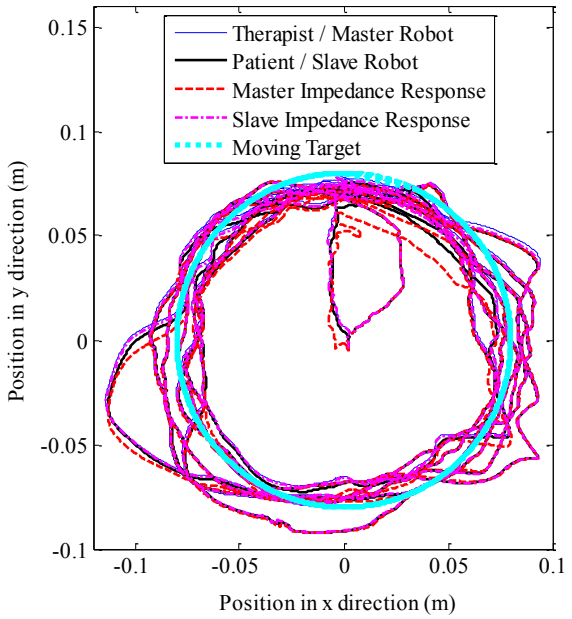

Fig. 7. Trajectories of the therapist, the patient and the master and slave impedance models responses in the $x-y$ plane during the tracking of the dynamic moving target in the cooperative tele-rehabilitation mode.

To show the varying velocity performance of the moving target, the magnitude of the target velocity and the patient distance with respect to the target (in the $x-y$ plane) are illustrated in Fig. 8. As it is seen, the velocity of the moving target increases as the patient's tracking error with respect to the target decreases.

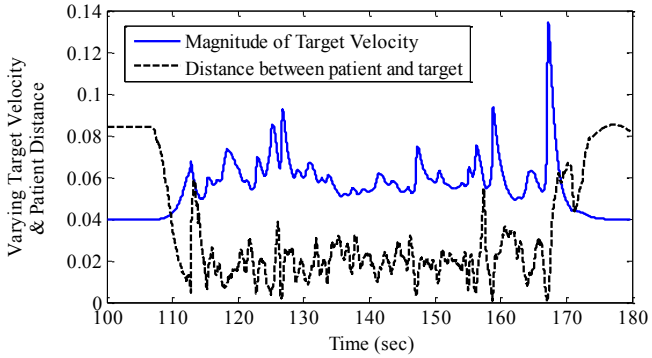

Fig. 8. The varying velocity of the moving target and the patient's distance with respect to the target (in the $x-y$ plane).

To elaborate more on the tracking performance, different position tracking errors are illustrated in Fig. 9. As it is observed, the master and slave control laws provide the tracking of the desired impedance responses ($\mathbf{x}_m \to \mathbf{x}_{\mathrm{mod}_m}$ and $\mathbf{x}_s \to \mathbf{x}_{\mathrm{mod}_s}$). Also, the difference between the desired slave impedance model's response and the master trajectory ($\tilde{\mathbf{x}}_{\mathrm{mod}_s} = \mathbf{x}_{\mathrm{mod}_s} - k_{\mathrm{p}}\,\mathbf{x}_m$) is small due to the employment of large impedance parameters (k_s, c_s and m_s) in the slave impedance model (10).

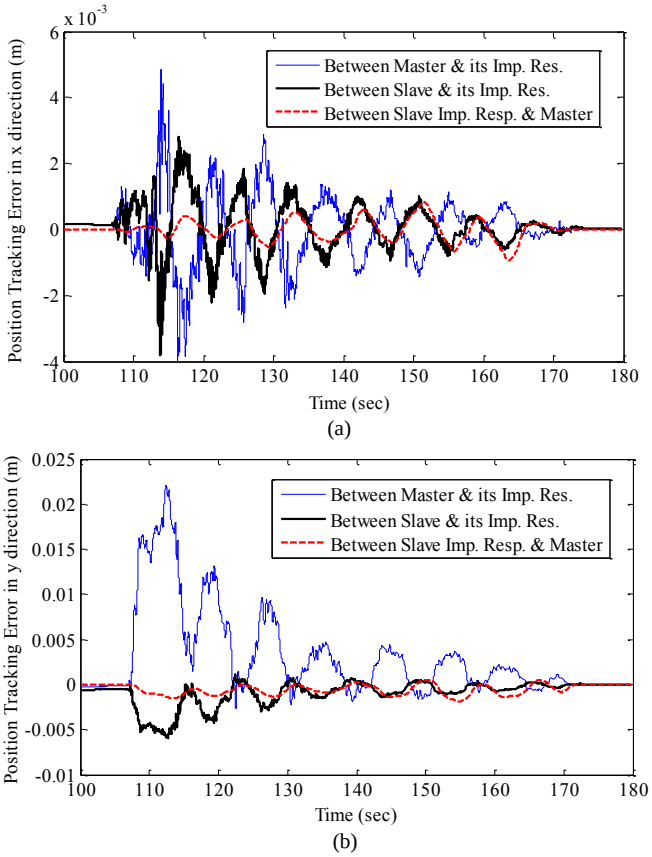

Fig. 9. Position tracking errors between the master and the slave and their reference impedance responses ($\tilde{\mathbf{x}}_m$, $\tilde{\mathbf{x}}_s$) and between the slave impedance response and the master ($\tilde{\mathbf{x}}_{\mathrm{mod}_s}$) in (a) x and (b) y directions.

Under this condition, the patient is restricted to have the same position as the therapist (as shown in Figs. 6 and 7), i.e., the patient is forced to comply with the therapist in tracking the moving target. However, in the next implemented strategy ("adjustable-flexibility" cooperative tele-rehabilitation), the patient can deviate from the therapist trajectory due to his/her forces.

Note that the results of "Hand-Over-Hand" cooperation mode (Figs. 5-7) became approximately compatible with the objectives of the Direct Force Reflection (DFR) control strategy [50] (which are the perfect position and force tracking instead of impedance adjustment). However, the DFR strategy

has the stability proof for a linear bilateral system [50], not for nonlinear systems used in the multi-DOF tele-rehabilitation.

6.2. "Adjustable-Flexibility" Cooperative Tele-rehabilitation Mode

In this section, the proposed bilateral impedance controller is evaluated when the patient has an adjustable flexibility with respect to the therapist/master trajectory. In other words, the slave impedance parameters in this tele-rehabilitation mode are smaller than the cooperative mode (previous section) as mentioned in Table 2.

As seen in Fig. 10, the force reflection performance ($\mathbf{f}_{th} - k_f \mathbf{f}_{pa} \to 0$) is achieved like the previous section of experiments (for cooperative mode), which is the result of choosing small master impedance parameters (k_m, c_m and m_m in Table 2). However, the patient position deviates from the therapist/master trajectory regarding to his/her applied force $\mathbf{f}_{pa}$ due to Eq. (10), as shown in Fig. 11. In this setting, the patient is assisted by the force exertions of the therapist on the master ($\mathbf{f}_{th}$ that is shown in Fig. 10 and affects $\mathbf{x}_{\mathrm{mod}_m}$ in Eq. (9) and consequently $\mathbf{x}_m$). The trajectories of the therapist, the patient and the impedance model responses together with the moving target one in the $x-y$ plane are illustrated in Fig. 12. As seen in Figs. 11 and 12, although the therapist physically tries with his/her force ($\mathbf{f}_{th}$ in Fig. 10) to encourage and assist the patient to accompany the moving target with circular path, the patient has a freedom and deviation ($\tilde{\mathbf{x}}_{\mathrm{mod}_s}$) from the therapist motion.

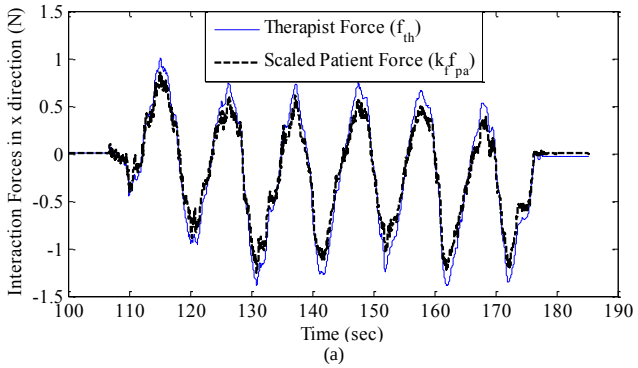

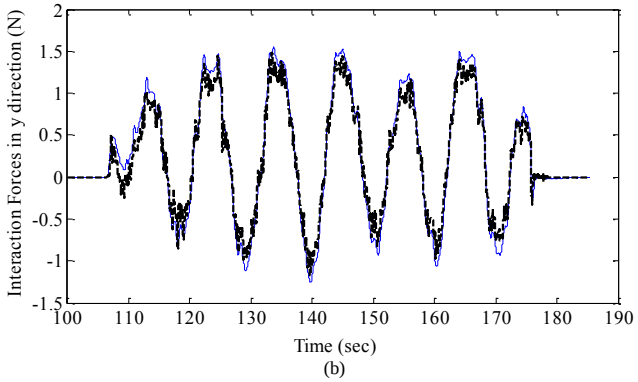

Fig. 10. The therapist and the scaled patient forces ($\mathbf{f}_{th}$ and $k_f \mathbf{f}_{pa}$) in (a) x and (b) y directions during the "adjustable-flexibility" cooperative tele-rehabilitation mode.

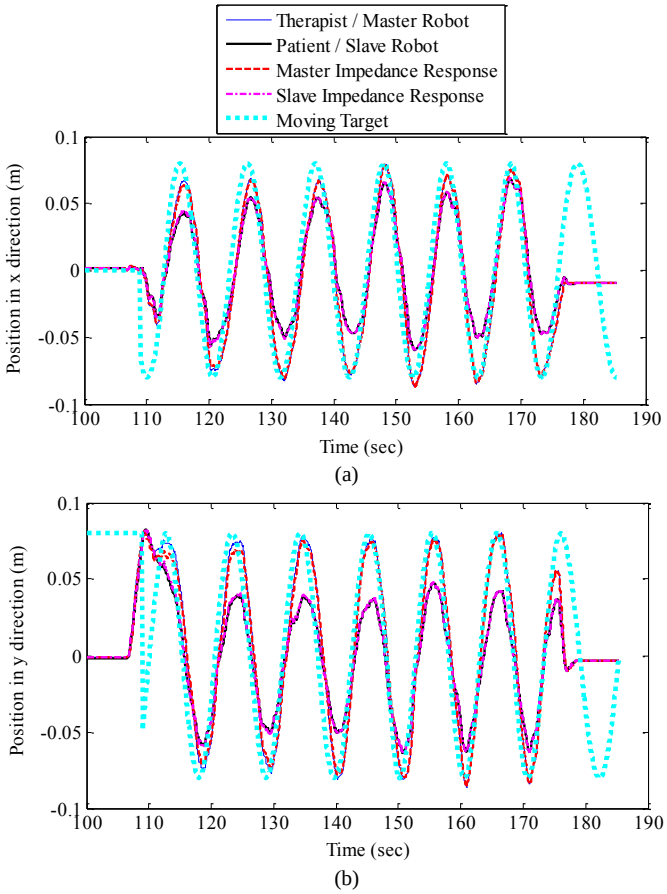

Fig. 11. The positions of the therapist's and the patient's hands with the master and slave impedance models responses in (a) x and (b) y directions, for the "adjustable-flexibility" cooperative tele-rehabilitation mode.

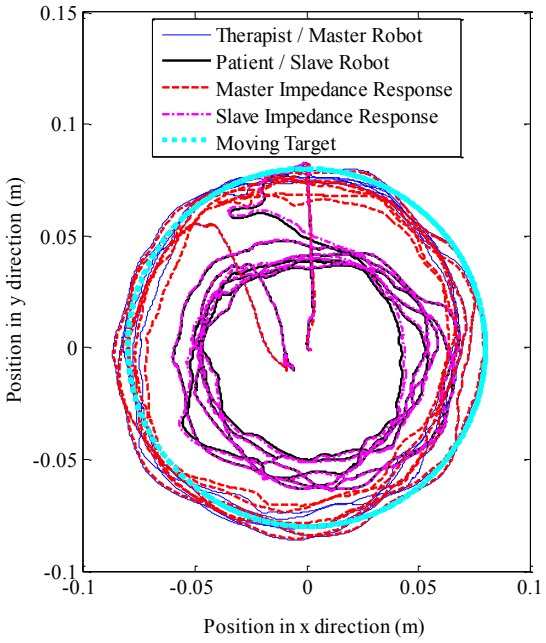

Fig. 12. Trajectories of the therapist, the patient and the master and slave impedance models responses in the $x-y$ plane during the tracking of dynamic moving target in the "adjustable-flexibility" cooperative tele-rehabilitation mode.

7. Discussion

As a useful feature of the proposed control strategy in tele-rehabilitation, the master and slave robots (interacting with the therapist and the patient, respectively) can have different force/torque rendering capabilities and also different workspace sizes due to the force and position scaling factors that are allowed. This feature can also reduce the therapist fatigue by reflecting scaled-down version of the patient force. Moreover, unlike the previous nonlinear bilateral adaptive controllers [29, 31, 41] in which force tracking was achieved only when the estimation of model parameters converged to the real values (persistent excitation condition), the position and force tracking have been obtained simultaneously in the current framework without any requirement on the precise identification of system parameters.

The design of proposed control laws for the master and the slave was motivated by a new nonlinear Model Reference Adaptive Impedance Control (MRAIC) [34] in order to make the closed-loop dynamics of robots similar to their corresponding stable reference impedance models. The stability of master and slave impedance models (9) and (10) was useful in the nonlinear bilateral MRAIC scheme; however, it can be a limitation of this bilateral controller. In other words, if unstable or marginally stable dynamics is considered as the reference impedance model for the master or slave robots in special cases, the proposed nonlinear control laws (17) and (18) should be modified appropriately such that the Lyapunov stability is still guaranteed.

The other limitation of the proposed tele-rehabilitation strategies may be the requirement of the therapist's force for physical assistance of the patient during movement therapies. However, an autonomous assistance can be defined in future works as the virtual therapist's force ($\mathbf{f}_{th}$ in Eq.(9)) in the absence of the human therapist's cooperation.

8. Conclusion

In this paper, a nonlinear bilateral impedance controller was designed with applications in cooperative tele-rehabilitation using two multi-DOF robot manipulators in a bilateral teleoperation configuration. The parameters of the two realized impedance models for the master and slave robots are adjusted to provide appropriate responses in each "hand-over-hand" and "adjustable-flexibility" tele-rehabilitation modes.

The stability of the master and slave impedance models together with the Lyapunov stability proof for the nonlinear multi-DOF robotic tele-rehabilitation system in the presence of modeling uncertainties guarantee the safety of the patient and the therapist during interaction with the robots.

The experimental evaluations using the multi-DOF Phantom Premium and Quanser Rehab Robots in different tele-rehabilitation modes showed the stability of the proposed controller and its impedance adjustment performance (i.e., success in realizing the desired impedance models for the master and slave robots). Following a moving target with a dynamically-varying velocity was designed as the patient's task in the cooperative tele-rehabilitation modes.

The objective of this work was evaluation of the proposed bilateral impedance controller in terms of facilitating cooperative tele-rehabilitation modes. However, more user studies involving patients with disabilities will be performed in the future. Moreover, the obtained force and position data

from the patient and therapist can be used in post-treatment analyses in order to quantify the patient performance or learning the therapist's behavior for reproduction in autonomous rehabilitation tasks (without the human therapist's real-time intervention). In future works, the patients improvements obtained using this strategy can be evaluated after a rehabilitation process in comparison with other ones obtained using traditional impedance controlled systems without the therapist assistance (by employing a single robot for the patient).

Acknowledgements

This research was supported by the Canada Foundation for Innovation (CFI) under grant LOF 28241; the Alberta Innovation and Advanced Education Ministry under Small Equipment Grant RCP-12-021; the Natural Sciences and Engineering Research Council (NSERC) of Canada under the Collaborative Health Research Projects (CHRP) Grant #316170; and the Quanser, Inc.

References

[1] A. A. Blank, J. A. French, A. U. Pehlivan, and M. K. O'Malley, "Current Trends in Robot-Assisted Upper-Limb Stroke Rehabilitation: Promoting Patient Engagement in Therapy," *Current Physical Medicine and Rehabilitation Reports*, vol. 2, pp. 184-195, 2014.

[2] H. I. Krebs and N. Hogan, "Robotic Therapy: The Tipping Point," *American journal of physical medicine & rehabilitation / Association of Academic Physiatrists*, vol. 91, pp. S290-S297, 2012.

[3] A. Gupta and M. K. O'Malley, "Design of a haptic arm exoskeleton for training and rehabilitation," *Mechatronics, IEEE/ASME Transactions on*, vol. 11, pp. 280-289, 2006.

[4] N. Hogan, H. I. Krebs, A. Sharon, and J. Charnnarong, "Interactive robotic therapist," ed: Google Patents, 1995.

[5] H. I. Krebs, B. T. Volpe, D. Williams, J. Celestino, S. K. Charles, D. Lynch, and N. Hogan, "Robot-Aided Neurorehabilitation: A Robot for Wrist Rehabilitation," *Neural Systems and Rehabilitation Engineering, IEEE Transactions on*, vol. 15, pp. 327-335, 2007.

[6] R. Riener, T. Nef, and G. Colombo, "Robot-aided neurorehabilitation of the upper extremities," *Medical and Biological Engineering and Computing*, vol. 43, pp. 2-10.

[7] A. Gupta, M. K. O'Malley, V. Patoglu, and C. Burgar, "Design, Control and Performance of RiceWrist: A Force Feedback Wrist Exoskeleton for Rehabilitation and Training," *The International Journal of Robotics Research*, vol. 27, pp. 233-251, 2008.

[8] C. R. Carignan and H. I. Krebs, "Telerehabilitation robotics: Bright lights, big future?," *Journal of Rehabilitation Research and Development*, vol. 43, pp. 695-710, 2006.

[9] M. Johnson, R. V. Loureiro, and W. Harwin, "Collaborative tele-rehabilitation and robot-mediated therapy for stroke rehabilitation at home or clinic," *Intelligent Service Robotics*, vol. 1, pp. 109-121, 2008.

[10] V. G. Popescu, G. C. Burdea, M. Bouzit, and V. R. Hentz, "A virtual-reality-based telerehabilitation system with force feedback," *Information Technology in Biomedicine, IEEE Transactions on*, vol. 4, pp. 45-51, 2000.

[11] D. J. Reinkensmeyer, C. T. Pang, J. A. Nessler, and C. C. Painter, "Web-based telerehabilitation for the upper extremity after stroke," *Neural Systems and Rehabilitation Engineering, IEEE Transactions on*, vol. 10, pp. 102-108, 2002.

[12] C. Jadhav and V. Krovi, "A Low-Cost Framework for Individualized Interactive Telerehabilitation," in *Engineering in Medicine and Biology Society. IEMBS '04. 26th Annual International Conference of the IEEE*, 2004, pp. 3297-3300.

[13] J. Kim, H. Kim, B. K. Tay, M. Muniyandi, M. A. Srinivasan, J. Jordan, J. Mortensen, M. Oliveira, and M. Slater, "Transatlantic Touch: A Study of Haptic Collaboration over Long Distance," *Presence: Teleoperators and Virtual Environments*, vol. 13, pp. 328-337, 2004.

[14] C. Basdogan, C. H. Ho, M. A. Srinivasan, and M. Slater, "An experimental study on the role of touch in shared virtual environments," *ACM Trans. Comput.-Hum. Interact.*, vol. 7, pp. 443-460, 2000.

[15] R. Tao, "Haptic Teleoperation Based Rehabilitation Systems for Task-Oriented Therapy," M.Sc. Thesis, Department of Electrical and Computer Engineering, University of Alberta, 2014.

[16] M. Shahbazi, S. F. Atashzar, M. Tavakoli, and R. V. Patel, "Therapist-in-the-Loop robotics-assisted mirror rehabilitation therapy: An Assist-as-Needed framework," in *Robotics and Automation (ICRA), IEEE International Conference on*, 2015, pp. 5910-5915.

[17] S. F. Atashzar, M. Shahbazi, M. Tavakoli, and R. V. Patel, "A new passivity-based control technique for safe patient-robot interaction in haptics-enabled rehabilitation systems," in *Intelligent Robots and Systems (IROS), 2015 IEEE/RSJ International Conference on*, 2015, pp. 4556-4561.

[18] C. R. Carignan and P. A. Olsson, "Cooperative control of virtual objects over the Internet using force-reflecting master arms," in *Robotics and Automation. ICRA '04. IEEE International Conference on*, 2004, pp. 1221-1226.

[19] M. Shahbazi, S. F. Atashzar, and R. V. Patel, "A framework for supervised robotics-assisted mirror rehabilitation therapy," in *IEEE/RSJ International Conference on Intelligent Robots and Systems (IROS)*, 2014, pp. 3567-3572.

[20] M. Shahbazi, S. F. Atashzar, M. Tavakoli, and R. V. Patel, "Robotics-Assisted Mirror Rehabilitation Therapy: A Therapist-in-the-Loop Assist-as-Needed Architecture," *IEEE/ASME Transactions on Mechatronics*, vol. 21, pp. 1954-1965, 2016.

[21] I. Sharifi, H. A. Talebi, and M. Motaharifar, "A framework for simultaneous training and therapy in multilateral tele-rehabilitation," *Computers & Electrical Engineering*, vol. 56, pp. 700-714, 2016.

[22] J. E. Colgate, "Robust impedance shaping telemanipulation," *Robotics and Automation, IEEE Transactions on*, vol. 9, pp. 374-384, 1993.

[23] L. Dongjun and P. Y. Li, "Passive bilateral feedforward control of linear dynamically similar teleoperated manipulators," *Robotics and Automation, IEEE Transactions on*, vol. 19, pp. 443-456, 2003.

[24] D. A. Lawrence, "Stability and transparency in bilateral teleoperation," *Robotics and Automation, IEEE Transactions on*, vol. 9, pp. 624-637, 1993.

[25] I. G. Polushin, P. X. Liu, C.-H. Lung, and G. D. On, "Position-Error Based Schemes for Bilateral Teleoperation With Time Delay: Theory and Experiments," *Journal of Dynamic Systems, Measurement, and Control*, vol. 132, p. 031008 (11 pages), 2010.

[26] N. Chopra, M. W. Spong, and R. Lozano, "Synchronization of bilateral teleoperators with time delay," *Automatica*, vol. 44, pp. 2142-2148, 2008.

[27] E. Nuño, R. Ortega, and L. Basañez, "An adaptive controller for nonlinear teleoperators," *Automatica*, vol. 46, pp. 155-159, 2010.

[28] Y. C. Liu and N. Chopra, "Control of semi-autonomous teleoperation system with time delays," *Automatica*, vol. 49, pp. 1553-1565, 2013.

[29] J. H. Ryu and D. S. Kwon, "A novel adaptive bilateral control scheme using similar closed-loop dynamic characteristics of master/slave manipulators," *Journal of Robotic Systems*, vol. 18, pp. 533-543, 2001.

[30] M. Sharifi, S. Behzadipour, and H. Salarieh, "Nonlinear Bilateral Adaptive Impedance Control With Applications in Telesurgery and Telerehabilitation," *Journal of Dynamic Systems, Measurement, and Control*, vol. 138, p. 111010 (16 pages), 2016.

[31] X. Liu and M. Tavakoli, "Adaptive inverse dynamics four-channel control of uncertain nonlinear teleoperation systems," *Advanced Robotics*, vol. 25, pp. 1729-1750, 2011.

[32] N. Hogan, "Impedance Control: An Approach to Manipulation: Part I---Theory," *Journal of Dynamic Systems, Measurement, and Control*, vol. 107, pp. 1-7, 1985.

[33] A. Abdossalami and S. Sirouspour, "Adaptive Control for Improved Transparency in Haptic Simulations," *Haptics, IEEE Transactions on*, vol. 2, pp. 2-14, 2009.
[34] M. Sharifi, S. Behzadipour, and G. Vossoughi, "Nonlinear model reference adaptive impedance control for human–robot interactions," *Control Engineering Practice*, vol. 32, pp. 9-27, 2014.
[35] H. I. Krebs, J. J. Palazzolo, L. Dipietro, M. Ferraro, J. Krol, K. Rannekleiv, B. T. Volpe, and N. Hogan, "Rehabilitation Robotics: Performance-Based Progressive Robot-Assisted Therapy," *Autonomous Robots*, vol. 15, pp. 7-20, 2003.
[36] A. Rubio, A. Avello, and J. Florez, "Adaptive impedance modification of a master-slave manipulator," in *Robotics and Automation. Proceedings. IEEE International Conference on*, 1999, pp. 1794-1799.
[37] R. V. Dubey, C. Tan Fung, and S. E. Everett, "Variable damping impedance control of a bilateral telerobotic system," *Control Systems, IEEE*, vol. 17, pp. 37-45, 1997.
[38] K. Hashtrudi-Zaad and S. E. Salcudean, "Analysis of Control Architectures for Teleoperation Systems with Impedance/Admittance Master and Slave Manipulators," *The International Journal of Robotics Research*, vol. 20, pp. 419-445, June 1, 2001.
[39] H. C. Cho and J. H. Park, "Stable bilateral teleoperation under a time delay using a robust impedance control," *Mechatronics*, vol. 15, pp. 611-625, 2005.
[40] J. J. Abbott and A. M. Okamura, "Pseudo-admittance Bilateral Telemanipulation with Guidance Virtual Fixtures," *The International Journal of Robotics Research*, vol. 26, pp. 865-884, 2007.
[41] X. Liu and M. Tavakoli, "Adaptive Control of Teleoperation Systems With Linearly and Nonlinearly Parameterized Dynamic Uncertainties," *Journal of Dynamic Systems, Measurement, and Control*, vol. 134, p. 021015 (10 pages), 2012.
[42] F. Hashemzadeh and M. Tavakoli, "Position and force tracking in nonlinear teleoperation systems under varying delays," *Robotica*, vol. 33, pp. 1003-1016, 2015.
[43] X. Liu, R. Tao, and M. Tavakoli, "Adaptive control of uncertain nonlinear teleoperation systems," *Mechatronics*, vol. 24, pp. 66-78, 2014.
[44] J. J. E. Slotine and W. Li, *Applied nonlinear control*. NJ, Englewood Cliffs: Prantice-Hall, 1991.
[45] M. Sharifi, S. Behzadipour, and G. R. Vossoughi, "Model reference adaptive impedance control in Cartesian coordinates for physical human–robot interaction," *Advanced Robotics*, vol. 28, pp. 1277-1290, 2014.
[46] W. S. Lu and Q. H. Meng, "Impedance control with adaptation for robotic manipulations," *Robotics and Automation, IEEE Transactions on*, vol. 7, pp. 408-415, 1991.
[47] M. C. Çavuşoğlu, D. Feygin, and F. Tendick, "A Critical Study of the Mechanical and Electrical Properties of the PHANToM Haptic Interface and Improvements for High-Performance Control," *Presence: Teleoperators & Virtual Environments*, vol. 11, pp. 555-568, 2002.
[48] M. D. Dyck, "Measuring the Dynamic Impedance of the Human Arm," M.Sc. Thesis, Department of Electrical and Computer Engineering, University of Alberta, 2013.
[49] M. Dyck and M. Tavakoli, "Measuring the dynamic impedance of the human arm without a force sensor," in *Rehabilitation Robotics (ICORR), IEEE International Conference on*, 2013, pp. 1-8.
[50] M. Tavakoli, *Haptics for teleoperated surgical robotic systems*. Hackensack, NJ: World Scientific, 2008.